SEARCH FOR A SUPERFLUID PHASE OF PARAHYDROGEN: EXPLORING THE EFFECT OF CONFINEMENT

by

Tokunbo P. Omiyinka

A thesis submitted in partial fulfillment of the requirements for the degree of

Doctor of Philosophy

Department of Physics

University of Alberta

Abstract

The first part of this thesis theoretically studies the low temperature physics of parahydrogen (p-H$_2$) confined in cylindrical channels of diameter of the order of 1 nm, based on the Continuous-Space Worm Algorithm quantum Monte Carlo simulations. On varying the attractive strength of the wall of the cylindrical pore, as well as its diameter, the equilibrium phase evolves from a single quasi-one-dimensional (1D) channel along the axis, to a concentric cylindrical shell. It is found that the quasi-1D system retains a strong propensity to crystallization, even though on weakly attractive substrates quantum fluctuations reduce somewhat such a tendency compared to the purely 1D system. No evidence of a topologically protected superfluid phase (in the Luttinger sense) is observed. Secondly, this research work explores the possibility of existence of a metastable superfluid phase of p-H$_2$ in the low temperature limit. It was found that any possible occurence of superfluidity in supercooled p-H$_2$ would have to be at a much lower temperature than 2 K. Furthermore, this thesis investigates how different p-H$_2$ is from a Bose system that possesses a metastable superfluid phase despite having a crystalline ground state. Finally, study is also carried out to elucidate the inherent distinctions between an hypothetical metastable p-H$_2$ liquid and a metastable ^{4}He liquid, underscoring the essential origin of the almost conclusive absence of superfluidity in any phase of p-H$_2$. Extensive discussions are also provided on the implications of this work for the possible existence of a bulk superfluid phase of parahydrogen.

Preface

The entirety of this thesis constitute the original thesis research of Tokunbo Omiyinka, under the supervision of Professor Massimo Boninsegni.

Chapter 3 of this work has been published as: Tokunbo Omiyinka and Massimo Boninsegni, "Enhanced superfluid response of parahydrogen in nanoscale confinement", Physical review B **90**, 064511 (2014).

Also, Chapter 4 has been published as: Tokunbo Omiyinka and Massimo Boninsegni, "Quasi-one-dimensional parahydrogen in nanopores", Physical review B **93**, 104501 (2016).

Acknowledgements

Table of Contents

List of Tables

List of Figures

Chapter 1

INTRODUCTION

Superfluidity is a macroscopic manifestation of quantum mechanics, a phenomenon in which a substance is capable of sustaining non-dissipative (*super*)flow. Superflow can in principle be observed in all three phases of aggregation of matter, namely liquid, solid and gas. However, it is most easily observed and/or intuitively pictured in the liquid phase. A superfluid liquid will remain in a state of persistent flow (if set in motion below a critical velocity) through a pipe, without dissipation, and will flow through constrictions that are impassable to the normal liquid without any measurable pressure difference. It would rise through the narrowest capillaries with a flow velocity that is independent of the pressure head, indicating its non viscous flow, and it possesses a high thermal conductivity, which increases as the temperature is lowered below the superfluid transition temperature, making it nearly impossible to set up a measurable temperature gradient across the superfluid liquid. There exist several spectacular manifestations of superfluidity in the liquid phase, for example the fountain effect [1].

Helium (He) is the only known naturally occurring substance that exhibits

superfluid behaviour, in its liquid phase. Under the pressure of its own vapour, He condenses into a liquid at a temperature of 4.2 K [2], and remains a liquid all the way to temperature $T = 0$ K, at pressures below 25 atm. It was independently discovered by Kapitza [3], and Allen and Misener [4], that the liquid phase of ^{4}He, which is the more abundant isotope, undergoes a continuous phase transition into a superfluid at a temperature $T_\lambda = 2.17$ K. The less abundant isotope, ^{3}He, also turns superfluid, but at a much lower temperature, of the order of a few mK.

According to a useful phenomenological model introduced by Tisza [5], which we utilize throughout this thesis, a superfluid below the transition temperature can be regarded as a mixture of two fluids, one that is *normal* and the other that is *superfluid*. The *normal* component carries entropy and is subjected to dissipation like an ordinary fluid, while the *superfluid* component has no entropy and is able to flow without dissipation. In a system that is translationally invariant, e.g. a liquid, the *superfluid fraction* ρ_S, namely the fraction of the system in the superfluid phase, tends to 100% as the temperature $T \to 0$ (it is of course zero above T_λ). By definition, $\rho_S + \rho_N = 1$, where ρ_N is the so called *normal fraction*.

Several decades of experimental and theoretical investigation have afforded a great amount of insight into the microscopic origin of superfluidity. In particular, it is now widely accepted [6] that, at least in three dimensions, superfluidity is intimately connected to a phenomenon called *Bose-Einstein Condensation* (BEC), which manifests in assemblies of indistinguishable particles of integer spin (Bosons). BEC is a collective low temperature phenomenon that consists of the occupation of the same *single-particle* quantum-mechanical state by a *finite fraction* of particles in the system. The connection between

BEC and superfluidity is the key to understanding the widely different superfluid transition temperatures of ^{3}He and ^{4}He. ^{3}He atoms have spin $1/2$, and therefore obey Fermi statistics. Thus, they are not able to undergo BEC by themselves. The formation of bound pairs of ^{3}He atoms of opposite spin projections, forming a composite object of spin 1, underlies occurrence of superfluidity, as these composite objects act in a sense as bosons and are therefore able to undergo BEC. Indeed superfluidity occurs in ^{3}He at a temperature which is of the order of the binding energy of two ^{3}He atoms in forming such bosonic pairs. Such a pairing mechanism is believed to underlie superfluidity in all Fermi systems, including superconductors, which are basically charged superfluids [1].

First principle computer simulations, based on the Path Integral formulation of quantum mechanics due to Feynman [7], have made it possible to achieve giant strides toward the clear understanding of superfluidity. Specifically, the subtle relationship between superfluidity and BEC has been well highlighted by the Path Integral Monte Carlo method [8], which has revealed unambiguously that the same effect which underlies BEC, i.e. formation of macroscopic exchange cycles of indistinguishable particles (helium atoms), is also responsible for superfluidity and that superfluid ^{4}He, in 3D, is indeed a Bose-Einstein condensate. There remain however some nontrivial outstanding issues. For example, the quantitative connection between superfluidity and BEC is still unclear; it is not understood whether BEC and superfluid transition should necessarily occur at the same temperature; also controversial is whether any Bose system escaping crystallization at low temperature should have a superfluid ground state [9].

Discovering superfluidity in another liquid of the simplicity and accessi-

bility of ^{4}He, might considerably strengthen the current microscopic under-standing of this phenomenon, insofar as it could help address the above issues, and others that still need to be elucidated. While it is true that superfluidity has been observed in cold atomic gases [10], that is a highly dilute system, in which the fraction of atoms in the Bose condensate is essentially 100% in the ground state. In that context, a relatively simple mean-field treatment furnishes a rather accurate account of the superfluid properties of the gas [10]. More interesting is the situation in a strongly interacting condensed matter *quantum fluid*, in which Bose Condensation is strongly reduced, such as in ^{4}He.

Among naturally occurring substances, molecular hydrogen, specifically *parahydrogen* (p-H$_2$) has long been regarded as the most plausible candidate to feature a superfluid phase at low temperature. Its elementary constituents are diatomic molecules of zero net spin, thereby obeying Bose statistics, of mass half that of a helium atom, i.e., quantum-mechanical effects should in principle be even more pronounced than in the condensed phase of ^{4}He. In fact, the prediction was first made over 40 years ago that a fluid of p-H$_2$ molecules should undergo a superfluid transition at a temperature around 6 K [11]. Such a prediction is based on a very simple model that regards a fluid of p-H$_2$ molecules as a non-interacting Bose gas, a crude assumption which nonetheless yields a surprisingly accurate estimate of the superfluid transition of liquid ^{4}He. A more realistic theoretical treatment, taking interparticle interactions into consideration, places the superfluid transition temperature of p-H$_2$ at around ~ 2 K [12, 13].

However such a hypothetical superfluid phase has so far eluded direct, unambiguous experimental observation. The problem with the original pre-

diction is that it assumes fluidlike behavior of p-H_2 at low T, when in fact the system undergoes crystallization (under the pressure of its own vapor) at $T = 13.8$ K, almost a factor 7 higher than the temperature at which Bose-Einstein Condensation and superfluidity ought to occur [14, 15]. Solidification results mostly because of the depth of the attractive well of the intermolecular potential, roughly three times that between two ^{4}He atoms.

If the propensity of p-H_2 fluid towards crystallization could be in some way suppressed, it is widely believed that p-H_2 would undergo a superfluid transition. Supercooling of fluid parahydrogen below its freezing temperature has been attempted experimentally, but it has so far not been possible to reach a temperature below ~ 9 K [16]. Reduction of dimensionality, disorder and confinement have long been regarded as plausible avenues to the stabilization of a fluid phase of p-H_2 down to temperatures sufficiently low that a superfluid transition could be observed. Reduction of dimensionality can lower significantly the freezing temperature, owing to the lower coordination number and the consequent lesser role played by the potential energy. The simplest way of achieving it experimentally consists of adsorbing a p-H_2 monolayer on a suitable substrate [17].

However, the zero temperature equilibrium phase of p-H_2 has been theoretically shown to be a (nonsuperfluid) crystal even in two and one dimensions, with no metastable fluid phase existing at T=0 K [18, 19].

The suggestion was made, almost two decades ago [20], that superfluidity might occur in a (quasi) two-dimensional p-H_2 fluid embedded in a crystalline matrix of alkali atoms. The contention was that the presence of the underlying lattice of foreign atoms, incommensurate with the equilibrium crystal structure of pure p-H_2, would cause the appearance of a new phase, presumed to be a

5

liquid on account of its much lower density than that of the equilibrium phase of p-H_2 in two dimensions. Numerical simulations appeared to support such a scenario, providing evidence of a superfluid transition at a temperature T close to 1 K. Subsequent studies [21, 22, 23], however, disproved such a prediction, showing it to be merely an artifact of simulations carried out on systems of extremely small size (about 10 particles). In actuality, the equilibrium phase is a non-superfluid crystal, commensurate with the underlying impurity lattice. A broader conclusion of those studies was that, although it is true that confinement and disorder can indeed lead to novel phases of matter, the strong propensity of p-H_2 to solidify renders it exceedingly unlikely that one may arrive at a superfluid phase in this way, as a commensurate crystal is the only additional phase that can result from the presence of an external periodic potential. The tendency of p-H_2 to crystallize is in fact so pronounced, that even on a disordered substrate the system forms an irregular (i.e., defect ridden) crystal [22].

Going back to three dimensions, one way of lowering the freezing temperature of a fluid is to confine it in a porous medium such as vycor glass [24, 25, 26]. In the pores of vycor, whose characteristic size [27] is $\sim$ 4 nm, p-H_2 freezes [28] at a temperature $T \sim 8$ K, considerably lower than that of bulk p-H_2, but still significantly above the estimated superfluid transition temperature; for this reason, the search for superfluid behaviour of p-H_2 in vycor has not met with success [29, 30].

It is worth noting that a) crystallization inside vycor glass originates at the surface of the pores [28], as the silica substrate acts as a strong attractor of p-H_2 molecules, and b) first principle theoretical simulations based on realistic intermolecular potential [31, 32, 33] yield evidence that small p-H_2 clusters

6

(thirty molecules or less), of typical size 1-2 nm, which remain liquidlike at low temperature, display superfluid behavior at a temperature of the order of 1 K; on the other hand, as the size of the clusters is increased, crystallization quickly sets in, with the concurrent suppression of superfluidity. Based on the above two observations, one is led to the speculation that different physics (possibly including a superfluid phase) may be observed in a different confining environment, e.g., with pores of smaller size (1-2 nm) and/or with a substrate less strongly adsorbing than silica.

The bulk of the research carried out during my Master's degree focused on the study of superfluidity of p-H_2 confined in weakly adsorbing spherical cavities of size 2 nm or less. The most important result is the theoretical prediction, based on computer simulations [34], that p-H_2 clusters of ~ 30 molecules confined in weakly adsorbing spherical cavities of size ~ 2 nm surprisingly feature an *enhanced* superfluid response compared to that of free clusters. It is therefore conceivable that the same effect may take place in a different geometry, e.g., cylindrical channels, experimentally relevant to actual porous media. One could therefore think of achieving a bulk superfluid response in a network of interconnected, quasi-one-dimensional channels of characteristic diameter 1-2 nm, made of the appropriate material.

As the diameter of the channel is reduced to one nm or less, the physics of a fluid confined in it approaches the 1D limit, and becomes therefore amenable to interpretation within the framework of Luttinger liquid theory (LLT) [35], as revealed by computer simulations of ^{4}He confined in nanopores of such a characteristic size [36]. Although no true superfluid order can exist in one dimension, there exists a well-defined theoretical scenario in which a 3D bulk superfluid phase may arise in a network of interconnected, quasi-1D chan-

7

nels [37, 38]. Such a scenario requires that the fluid inside the channel be a superfluid, in some specific (Luttinger) sense which will be described later on.

The first part of this thesis consists of the theoretical exploration, by means of Quantum Monte Carlo simulations, of the phase diagram of a quasi-1D fluid of p-H_2 in the narrow confines of a cylindrical channel of diameter of the order of 1 nm. The hypothesis being probed here is whether quantum excursions of molecules in the direction perpendicular to the axis of the cylinder, which act to screen the intermolecular potential, may act to the point of reducing the propensity of the system to form a crystal, possibly stabilizing a superfluid phase, in the Luttinger sense. Our results show that confinement of p-H_2 in relatively weak cylindrical channels (alkali metals) leads to stable quasi-1D phases with much reduced propensity to crystallize. While this outcome is qualitatively consistent with the previously reported [34] enhancement of superfluid response of p-H_2 inside spherical cavity, quasi-1D p-H_2 remains insulating in the Luttinger sense. The main consequence is that the superfluid "Shevchenko state" scenario does not appear feasible for p-H_2 in porous media.

In the second part of the thesis, the more general question is addressed of the possibility of existence of a metastable superfluid phase of p-H_2 at low temperature. First, we present results of simulations of supercooled liquid p-H_2 down to a temperature $T = 3$ K, showing no evidence of incipient superfluid behaviour. Specifically, the extreme infrequency with which permutations of identical particles occur, known to underlie superfluidity, yields strong evidence that a superfluid transition, if it occurs at all in supercooled p-H_2, likely takes place at a significantly lower temperature than presently estimated.

The general conditions are then investigated for the existence of a metastable superfluid phase in the low temperature limit in a Bose system whose ther-

modynamic ground state is a crystal, if it is "stretched" to lower density than its equilibrium one (i.e., at negative pressure). The purpose of this study is to see how far p-H_2 is, in the space of interaction parameters, from a system that possesses a metastable superfluid phase despite having a crystalline ground state. In this context, the Lennard-Jones pair potential is used as a model interaction. The results of this study may be relevant to the present investigation of superfluidity in the context of cold atoms, where the interaction between individual particles can be "tuned" by means of mechanism such as the Feshbach resonance [39].

The remainder of this thesis is organized as follows: In the next chapter, a description is provided of the computational methodology adopted in this research work, and some of the basic terminology regarding the microscopic model(s) utilized in the various studies is introduced. Chapter three summarizes the main results of the studies that precede and are propaedeutic to the investigation described in the present work; such studies constitute the bulk of my Master's thesis [40]. Specifically, the results of the study of p-H_2 trapped inside nanoscale size spherical cavities show that it is indeed possible to have robust superfluid response in p-H_2 in a confining medium. A detailed description of the results of the simulations of quasi-one-dimensional parahydrogen in cylindrical channels, which constitute a central result of my doctoral research, is offered in Chapter 4. In Chapter 5, results are shown of the simulation of supercooled liquid parahydrogen down to temperatures where the hypothetical superfluid transition should take place, not showing any presence of superfluid behaviour. This study definitively revises previous estimates furnished in the literature. Finally, the study of the phase diagram of Lennard-Jones fluids at T=0 K is illustrated. Concluding remarks are offered in the last Chapter,

where the implications of the findings of this work on the possible observation of a bulk superfluid phase of parahydrogen are discussed.

Chapter 2

METHODOLOGY

In this chapter, we present details of the computational approach adopted in our study of *para*-hydrogen in both bulk and in confinement.

2.A The Many-body Hamiltonian

Our system of interest consists of N p-H_2 molecules, regarded as pointlike particles of mass m and spin zero, hence obeying Bose-Einstein statistics. In a typical simulation, particles are enclosed in a vessel, shaped like a parallelepiped, and periodic boundary conditions are applied in all three directions [41]. Periodic boundary conditions are unnecessary whenever the system of interest is inherently finite, and that is the case for a cluster of molecules in confinement, whose study is described in the next chapter.

The many-body Hamiltonian of the system utilized in all of the studies carried out in this work is the following:

$$\hat{H} = -\lambda \sum_i \nabla_i^2 + \sum_{i<j} v(r_{ij}) + \sum_i V(\mathbf{r}_i). \tag{2.1}$$

Here, $\lambda \equiv \hbar^2/2m = 12.031$ KÅ^2, $r_{ij} \equiv |\mathbf{r}_i - \mathbf{r}_j|$ is the distance between any two p-H$_2$ molecules and $\mathbf{r}_i$ is the position of the ith molecule. The potential v describes the pair-wise interaction of p-H$_2$ molecules, whereas V that of p-H$_2$ molecules with a specific confining agent. While the latter depends on the geometrical and physical details of confinement, and therefore takes on a different expression depending on the specific physical settings in which one is interested, v is always the same in all of the studies carried out in this work. Because p-H$_2$ molecules are to a good approximation spherical objects, the approximation is normally made of regarding v as a central potential, i.e., only depending on the relative distance between two molecules.

The simplest expression that one can use for v is the so-called Lennard-Jones interaction, which captures all of the minimal, essential features of essentially *any* intermolecular or interatomic interaction:

$$v(r) = 4\varepsilon \left[\left(\frac{\sigma}{r} \right)^{12} - \left(\frac{\sigma}{r} \right)^6 \right] \qquad (2.2)$$

In the above equation, σ can be roughly physically understood as the minimum distance down to which two molecules can be brought before a strong repulsion sets in, whose physical origin is quantum-mechanical, namely the Pauli exclusion principle, acting so as to prevent electronic clouds of different molecules from overlapping spatially. At large interparticle separation, the potential is weakly attractive and asymptotically tends to zero as $1/r^6$, as a consequence of the attraction between the mutually induced electric dipoles associated to the two molecules [42].

Expression (2.2) has a minimum at an interparticle separation $r \sim 1.12\ \sigma$, where the potential is worth $-\varepsilon$, i.e., the quantity ε is the depth of the at-

tractive well of the potential. Such a distance is that at which two nearest-neighboring particles would sit in the classical (crystalline) ground state of the system. The accepted values of these two parameters for the interaction between two p-H$_2$ molecules are $\sigma = 2.96$ Å, $\varepsilon = 34.16$ K [43].

Although the potential (2.2) does capture the basic physical features of the interaction between two p-H$_2$ molecules, more elaborate potentials must be used if one is seeking quantitative agreement with experiment. To that aim, more accurate expressions have been developed, among which that of Silvera and Goldman [44] has been most commonly utilized in theoretical studies of the condensed phases of p-H$_2$. Although such a potential is reasonably accurate in reproducing the physical properties of p-H$_2$ in the equilibrium solid phases, it proves increasingly less reliable as the system is pressurized. In a study like that carried out here, this can be a potentially serious shortcomings, as the interest here is that of elucidating the nature of the thermodynamic phases of p-H$_2$ in tight (nanoscale size) confinement, wherein the density of p-H$_2$ is not uniform, and it could be quite high in the vicinity of the surface, e.g., in case of a strongly attractive substrate. It makes therefore sense to utilize a pair potential that is more accurate at high pressure than the standard Silvera-Goldman pair potential.

In all of the studies described here, use is made of a refinement of a potential recently proposed by Moraldi [45]. Obtaining such a refinement, which eliminates some unphysical features of the potential originally proposed by Moraldi, constituted a major portion of the work carried out in my Master's thesis [40]. The modified pair potential was shown [46] to reproduce rather accurately the experimental equation of state of solid p-H$_2$, up to megabar pressure.

2.B The Continuous-space Worm Algorithm

The Path Integral Monte Carlo (PIMC) technique is the most reliable computational method for computing accurate thermodynamic properties of Bose systems at finite temperature. In particular, it has proven an immensely valuable tool to elucidate the connection between superfluidity and Bose-Einstein condensation [8]. Our calculations exclusively utilize Path Integral Monte Carlo (PIMC) simulations based on the Continuous Space Worm Algorithm [47, 48]. The PIMC approach involves implementing the Feynman's Path Integral [49] space-time approach to quantum statistical mechanics through a suitable Monte Carlo strategy. The PIMC scheme is at least in principle numerically exact, and has no adjustable parameter, taking the microscopic Hamiltonian as its only input. It also does not have any inherent bias, since no *a priori* assumption is made on the physics of the system, e.g., a trial wave function is not needed. The methodology is numerically exact for Bose systems. For Fermi systems, not considered in this work, it is only approximate.

2.B.1 Thermal Averages and Path Integration

The thermal average of a physical observable, for an N-particle system described by Eq. (2.1) at temperature T, represented by an operator $\hat{\mathcal{O}}$, is given by

$$\langle \hat{\mathcal{O}} \rangle = \frac{\mathrm{Tr}\,(\hat{\mathcal{O}}\hat{\rho})}{\mathrm{Tr}\,\hat{\rho}} = \frac{\int dR\,\mathcal{O}(R)\rho(R,R,\beta)}{\int dR\,\rho(R,R,\beta)} \tag{2.3}$$

where $R \equiv \mathbf{r}_1\,\mathbf{r}_2 \ldots \mathbf{r}_N$, i.e, the positions of all the N particles in the N-particle configuration and $\beta = 1/(k_B T)$. Henceforth, we shall set $k_B = 1$. For all cases of practical relevance in this work, the observable $\hat{\mathcal{O}}$ only depends

on the positions of all (or some) the particles in the system. The many-body density matrix, $\rho(R, R', \beta)$, is given by

$$\rho(R, R', \beta) = \langle R | e^{-\beta \hat{H}} | R' \rangle \tag{2.4}$$

with $\hat{H}$ being the quantum-mechanical many-body Hamiltonian of Eq. (2.1) while the *partition function*, which is the trace of the many-body density matrix, is given by

$$Z = \int dR \, \rho(R, R, \beta) \,.$$

The many-body density matrix is not usually known and Eq. (2.3) is evaluated through the path integration procedure prescribed by R. P. Feynman in 1948. Accordingly, the partition function is given by

$$Z = \int \mathcal{D}R(u) \, \exp\left\{-\mathcal{S}[R(u)]\right\} \,. \tag{2.5}$$

The integration in Eq. (2.5) is performed over all possible continuous, β-periodic N-particle configuration paths $R(u)$, i.e., $R(u) \equiv \mathbf{r}_1(u) \, \mathbf{r}_2(u)...\mathbf{r}_N(u)$, the quantity $0 \leq u\hbar \leq \beta\hbar$ typically being referred to as "imaginary time". Paths are β-periodic, i.e., $R(0) = \mathcal{P}R(\beta)$, namely the positions of all the particles at $u = 0$ and those at $u = \beta$ are the same, except for a possible permutation $\mathcal{P}$ of particle labels at $u = \beta$. $\mathcal{S}[R(u)]$ is the so-called Euclidean action of a given path, expressed as

$$\mathcal{S}[R(u)] = \int_0^\beta du \left\{ \sum_{i=1}^N \frac{m}{2\hbar^2} \left(\frac{d\mathbf{r}_i}{du}\right)^2 + \mathcal{V}(R(u)) \right\} , \tag{2.6}$$

15

where $\mathcal{V}(R(u))$ is the total potential energy of the system at the configurations visited along the path. The Euclidean action is related to the balance between *kinetic* (path curvature) and *potential* energy, which depends on interactions, along the various paths. Generally, smooth, straight paths have higher probability while paths of high potential energy have lower probability [49].

2.B.2 PIMC and Quantum Statistics

The evaluation of the thermal average, (2.1) is most suitably achieved through a Monte Carlo strategy. This involves employing the Metropolis Algorithm [50] to sample many-particle paths $R(u)$ through configuration space, based on a probability distribution proportional to $\exp[-\mathcal{S}(R(u))]$. Thermal expectation values, such as (2.1), are then calculated as *statistical* averages of the physical observable of interest along paths.

The calculation of the action integral involves time discretization, which inevitably leads to a time-step error, like in most numerical schemes; this can however be made arbitrarily small, provided enough computer time. Thus, one considers discrete paths $R(u) \equiv \{R_0, R_1, \ldots, R_{M-1}\}$ for a finite number M of "time slices". The imaginary "time step" τ is defined through $M\tau = \beta$. The simplest approximate action (due to path discretization) is given by (with an obvious notation)

$$\mathcal{S}[R(u)] \approx \sum_i^N \sum_{l=0}^{M-1} \frac{m(\mathbf{r}_{il} - \mathbf{r}_{il+1})^2}{2\tau\hbar^2} + \tau \sum_{l=0}^{M-1} \mathcal{V}(R_l). \qquad (2.7)$$

The probability with which a discrete path $R(u)$ is sampled is then given by

$$P \propto \exp\left\{-\mathcal{S}[R(u)]\right\} = \prod_{i=1}^{N}\prod_{l=0}^{M-1} \rho_\circ(\mathbf{r}_{il}, \mathbf{r}_{il+1}, \tau) \times \prod_{l=0}^{M-1} \mathrm{e}^{-\tau V(R_l, \tau)} \qquad (2.8)$$

where

$$\rho_\circ(\mathbf{r}, \mathbf{r}', \tau) = \left(2\pi\hbar^2\tau/m\right)^{-d/2} \exp\left[-\frac{m(\mathbf{r}-\mathbf{r}')^2}{2\hbar^2\tau}\right] \qquad (2.9)$$

is the density matrix for a free particle, where d is the dimensionality of the system (d is always equal to three in this work). The discrete action becomes exact in the limit $M \to \infty$.

As previously mentioned, quantum statistics, i.e, particle indistinguishability, is effected in the above formalism by allowing $R(\beta{=}M\tau) = \mathcal{P}R(0)$, the permutation $\mathcal{P}$ implying that, while actual positions occupied by particles in $R(\beta)$ and $R(0)$ are the same, particles are allowed to trade place. This reproduces the necessary symmetrization of the many-body density matrix, Eq. (2.4), i.e., it results in,

$$\rho(R, R', \beta) = \frac{1}{N!}\sum_{\mathcal{P}} \eta^{\mathcal{P}} \rho(R, \mathcal{P}R', \beta) \qquad (2.10)$$

where $\eta = +1$ for Bosons, -1 for Fermions. This is a crucial ingredient in quantum statistical mechanics; in Bose systems, as mentioned above, permutations underlie phenomena such as Bose condensation, whereas in Fermi systems particle indistinguishability results in the existence of a Fermi surface in normal Fermi liquids. The sampling of many-particle paths which allows particles to "trade place" as described, can be formally accomplished quite straightforwardly using the methodology described below. The two different types of

17

quantum statistics, however, lead to very different implementation issues, as will be clarified below.

Finally, the thermal expectation of a physical observable $\mathcal{O}$, given by Eq. (2.3), is then evaluated as

$$\langle \hat{\mathcal{O}} \rangle \sim \frac{\sum_{paths} \eta^{\mathcal{P}} \mathcal{O}(R_{path})}{\sum_{paths} \eta^{\mathcal{P}}} \tag{2.11}$$

where $\mathcal{P}$ is the parity of the permutation associated with particle relabelling (exchange), $\mathcal{O}(R_{path})$ is the average value of $\mathcal{O}$ along a path and, as before, $\eta = +1$ for Bose , -1 for Fermi statistics.

The direct averaging over paths as expressed in Eq. (2.11) becomes exponentially intractable with increasing N for Fermi systems at low temperature, when contributions from paths in which particles permute become important; for, the sum over paths comprises in that limit "*an alternating series of terms of opposite signs*", which very nearly cancel each other out [51]. As one is attempting to evaluate numerically the ratio of two exponentially small quantities, one encounters a very low "signal-to-noise" ratio, rendering the calculation not feasible in practice at low temperature, for system comprising more than just a few particles. For Bose systems, on the other hand, $\eta = +1$, and therefore no such problem arises. Because in this work we are only concerned with Bose systems, we shall make no further mention of the above difficulty, referred in the literature as "sign problem of quantum Monte Carlo".

2.B.3 Thermal Wavelength and Particle Permutations

Although in principle permutations of identical particles should always be taken into account, in practice at sufficiently high temperature only the iden-
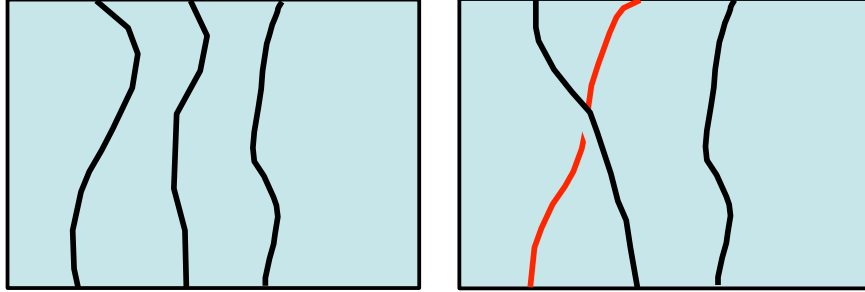
Figure 2.1: Permutation sampling in conventional PIMC

tity permutation (i.e., the one with $\mathbf{r}(\beta) = \mathbf{r}(0)$) will yield a significant contribution. Permutations of identical particles become increasingly important as $T \to 0$, and it is relatively simple to estimate the "degeneracy temperature", namely that below which permutations can be expected to yield a significant contribution. The characteristic "size" of a single particle path is measured by the thermal wavelength

$$\lambda_T = \frac{\hbar}{\sqrt{mT}}$$

Permutations can occur when λ_T is of the order of the mean interparticle distance i.e, $T \sim \hbar^2 n^{2/d}/m$, where n is the particle density.

2.B.4   Permutation Sampling In PIMC

Sampling of configurations (i.e., many-particle paths) in PIMC is achieved by implementing moves in configuration space; each move modifies the current configuration, i.e., the set of N world lines, and creates a "trial" new one, which is accepted or rejected according to the Metropolis recipe. The simplest moves are those that involve the path of a single particle, and are reminiscent of those implemented in classical (e.g., polymer) systems. Sampling of many-particle permutation paths, on the other hand, is an essential ingredient of

a *bona fide* quantum simulation, especially when effects of quantum statistics are of interest. Thus, basic to an effective Monte Carlo implementation of the Path Integral formalism is an efficient scheme of sampling permutations [8]. The path sampling procedure in the simplest implementation of PIMC, as described, for instance, in Ref. [52], is achieved through elementary moves that modify portions of single-particle paths. In particular, permutations are sampled by explicit construction of permutation cycles. As depicted in Fig. (2.1), this involves disconnecting the world lines of individual particles in pairs and attempting to reconnect them together to achieve exchanges of particles (figure shows a two-particle permutation). However, in the presence of any realistic interaction potential, typically possessing a "hard" repulsive core, any such sampling of permutations is bound to have high likelihood of rejection and therefore becomes inefficient. Rejection occurs because the constructed trial path will almost always bring two particles within near vicinity of each other, i.e, the trial configuration will have high potential energy. In practice, efforts required to sample macroscopic permutation cycles scales exponentially with the system size. This challenge limits the number of particles for which the low temperature thermodynamics of a system can be effectively studied, making accurate extrapolation of results to the thermodynamic limit highly problematic, using the conventional PIMC implementation. The conventional PIMC implementation also does not allow for the simultaneous evaluation of diagonal and off-diagonal correlations, as its configuration space only contains closed world lines (particle paths).

2.B.5 Effective Permutation Sampling: The Worm Algorithm

The Worm Algorithm completely resolves the issues mentioned above. A fundamental feature of the continuous-space worm algorithm is that it functions in an extended configurational space, including both closed world line configurations, referred to as the Z-sector, as well as configurations having one open world line (worm), known as the G-sector. A schematic view of the G-sector of the configuration space of the worm algorithm is seen in Fig. (2.2) (from Ref. [48]). The Worm Algorithm simultaneously accumulate statistics for diagonal (Z-sector) and off-diagonal (G-sector) correlations at no additional computational cost with respect to the simpler algorithm. All non-trivial topological modifications of the world lines that leads to long permutation cycles are intrinsically achieved through the G-sector. Closed
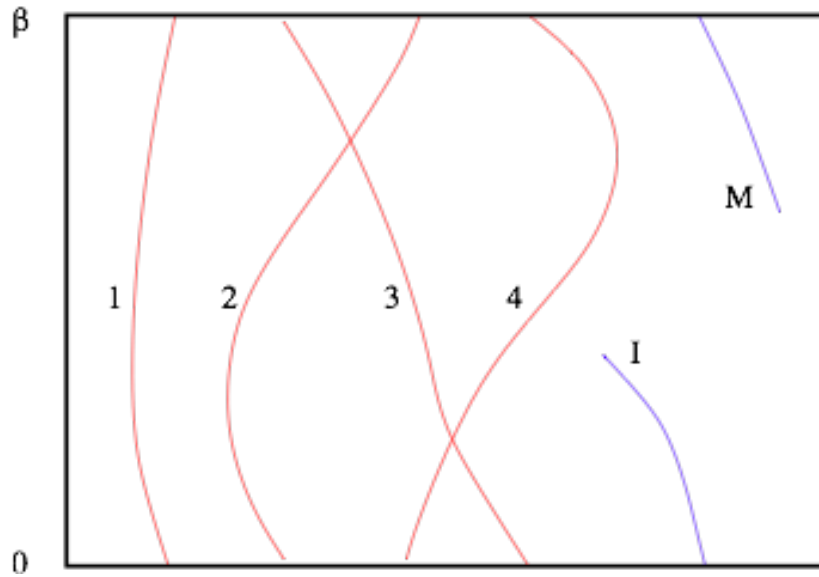
Figure 2.2: A sample of the Configuration space G-sector

.

world line configurations of the worm algorithm contribute to the partition

function, while configurations with an open world line, the *worm*, contribute to the one-particle *Matsubara Green function.* The *worm* is an open world line with two dangling ends which are referred to as Ira and Masha, denoted by $\mathcal{I}$ and $\mathcal{M}$ respectively in Fig. (2.2). The one-particle *Matsubara Green function* is expressed as

$$G(\mathbf{r}_1, \mathbf{r}_2, \tau) = \langle \hat{\mathcal{T}}[\hat{\psi}(\mathbf{r}_1, \tau)\hat{\psi}^{\dagger}(\mathbf{r}_2, 0)]\rangle . \qquad (2.12)$$

where $\hat{\psi}^{\dagger}$ and $\hat{\psi}$ are time-dependent Bose field operators, $\hat{\mathcal{T}}$ is the time ordering operator, $-\beta \leq \tau \leq \beta$. In the $\tau \to 0$ limit, the one-particle Matsubara Green function reduces to the one-particle density matrix, $n(\mathbf{r}_1, \mathbf{r}_2)$, from which the momentum distribution is computed [48] directly in the continuous-space Worm Algorithm.

The Worm Algorithm accurately calculates various thermodynamic quantities of interest for large Bose systems in easily accessible computation time. These quantities include the energetics, structure, superfluid density, condensate fraction, one-body density matrix and momentum distribution. Another elegant feature of the Worm Algorithm is that it can be implemented in either a canonical or a grand-canonical ensemble (resulting from fluctuations of particle number through annihilation and creation of worms).

In our current application of the Worm Algorithm, the Z-sector configurations have a fixed number N of particles, while configurations in the G-sector are constrained to having $N - 1$ particle world lines and a single worm. For details, the reader is referred to Refs. [47, 48].

Having utilized the Worm Algorithm to obtain a statistically representative set of space-time configurations of the quantum-mechanical system of interest, which are drawn from the appropriate probability distribution (Eq. (2.8)), one

becomes fully equipped to accurately compute the thermodynamic properties of the system. The estimation of the thermodynamic average of quantities that merely depend on the positions of the particles is straightforward, and carried out like in classical simulations [41]. For other quantities, appropriate estimators must be utilized (for details, see, for instance, Ref. [52]).

Estimation of the statistical uncertainty instrinsically associated to the evaluation of any physical average through Monte Carlo sampling has been carried out using the blocking/bunching method [53].

Chapter 3

ENHANCEMENT OF SUPERFLUID RESPONSE OF PARAHYDROGEN IN NANOSCALE CONFINEMENT

3.A Introduction

This chapter summarizes the main conclusions of the numerical simulations of parahydrogen clusters in nanoscale spherical confinement, carried out as part of my Master's thesis [40]. The most significant outcome of this study, which is propaedeutic to subsequent (doctoral) research work, is the observation of an enhanced superfluid response of p-H_2 clusters of size up to 2 nm when confined in spherical cavities with weakly attractive walls, with respect to
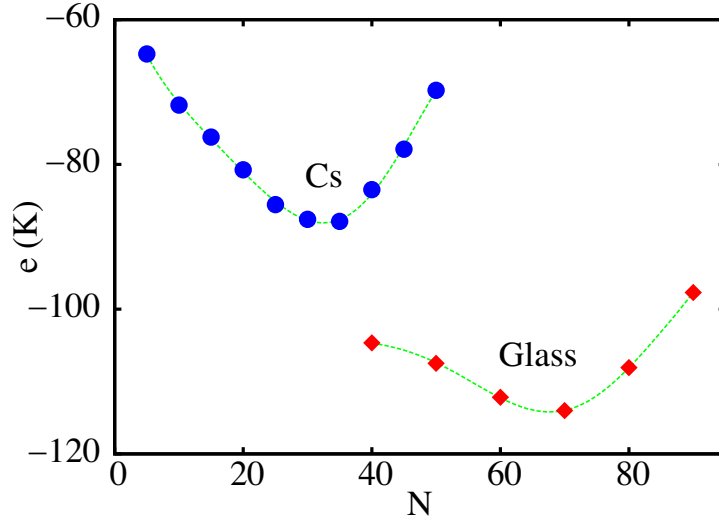
Figure 3.1: Energy per hydrogen molecule e (in K) versus number N in the $T \to 0$ limit, inside a Cs (filled circles) and glass (diamonds) cavities of radius 10 Å. Dashed lines are fits to the data. Statistical errors are at the most equal to symbol size.

their free counterparts. Illustrated below are two sets of simulation results, both obtained by setting the cavity radius R to 10 Å, but with two distinct choice of substrates, namely Cs and glass. For details of the model utilized in the simulations, the reader is referred to Refs. [34, 40].

3.A.1 Energetics

Fig. 3.1 displays the ground state [54] (i.e., $T = 0$) energy per p-H_2 molecule (in K) as a function of the number of molecules in the cavity. Both curves feature minima at specific number of molecules, which correspond to the minimum number of molecules that fills the cavity, at thermodynamic equilibrium. The curve for glass is shifted some 30 K downward with respect to that for Cs, and its minimum is attained for a value of N close to seventy molecules, over twice as much as the corresponding one for a Cs cavity. This
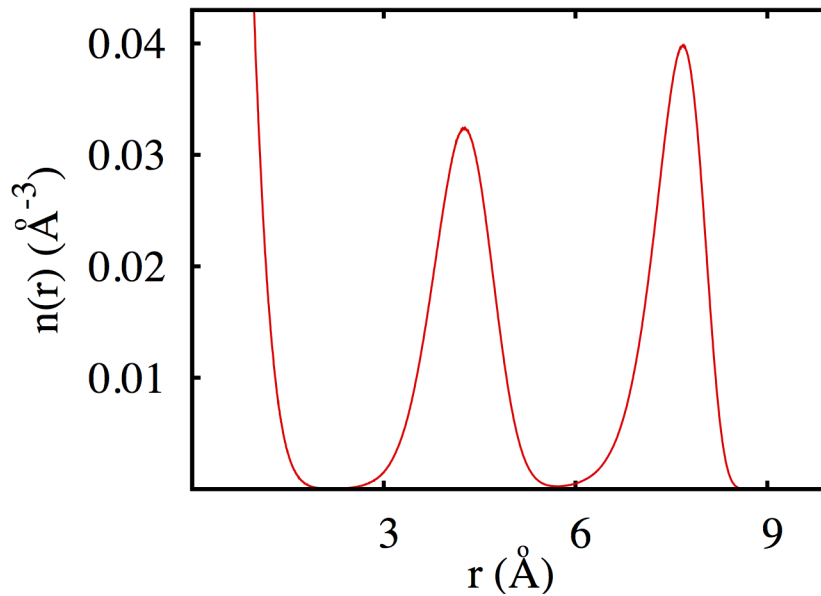
Figure 3.2: Radial density profile $n(r)$ in (Å^{-3}) for 70 p-H_2 molecules inside a glass cavity at $T = 0.5$ K, modeled as explained in the text. The strong peak at the origin signals the presence of a particle at the center of the cavity. Statistical errors are not visible on the scale of the figure.

is certainly consistent with the greater adsorption exerted by the glass cavity, and gives us an idea of the range within which N can vary inside a cavity of this size. An interesting thing to note is that for a Cs cavity, the minimum occurs at an energy close to -88.5 K, identical to the ground state chemical potential [40] for solid p-H_2. This implies that a cavity of this size is barely at the wetting threshold for a weakly adsorbing substrate such as Cs.

26

3.A.2 Structure of p-H$_2$ cluster in confinement

Glass cavity

In order to gain insight on the structure of p-H$_2$ inside the cavity, we examine the computed spherically averaged radial density of molecules $n(r)$, as a function of the distance from the centre of the cavity. Fig. 3.2 shows this quantity at $T = 0.5$ K for the case of seventy molecules inside the glass cavity. Density profiles for systems of sixty and fifty molecules in the glass cavity look very similar, the heights of the two peaks shown in Fig. 3.2 being slightly reduced. The density profile shows that molecules are arranged on concentric spherical shells, corresponding to the sharp density peaks. The half width of these peaks is less than 1 Å, i.e., shells are rigid, molecular excursions in the radial direction being fairly limited. This is true even within the shells, as molecules are scarcely mobile, held in place by the hard core repulsion of the intermolecular potential, which dominates the physics of the system at such dense parking. Consequently, quantum mechanical exchanges of molecules, which underlie the superfluid response in a quantum many-body system of indistinguishable particles, are strongly suppressed, and no appreciable superfluid response is obtained in this case.

Cesium cavity

A very different physical scenario, than in the glass cavity, takes place in the Cs enclosure, as shown in Fig. 3.3. Solid line shows the density profile for a cluster of 32 molecules, i.e., the minimum of the energy curve in Fig. 3.1, at $T = 1$ K. Also shown (dashed line) is the density profile for the same number of molecules in a glass cavity. There is a clear difference between the

Figure 3.3: Radial density profile $n(r)$ in (Å^{-3}) for 32 p-H_2 molecules inside a Cs cavity (solid line) at $T = 1$ K, modeled as explained in the text. Also shown are the profiles for the same number of molecules inside a glass cavity (dashed line) and in a free standing p-H_2 cluster (dotted line). Statistical errors are small on the scale of the figure.

arrangements of the p-H_2 molecules in the various cases; in the glass cavity, all the molecules are close to the surface, whereas in the Cs one they form two concentric shells, the outer sitting considerably closer to the centre of the cavity, and further away from its surface. This is, obviously, a consequence of the weakness of the Cs substrate compared to the glass one, and of the consequent greater importance of the role played by the repulsive core of the intermolecular potential at short distances.

Another important feature is that, unlike in the case shown in Fig. 3.2, the demarcation between the two shells present in the Cs cavity is not nearly

as sharp as in the glass one, as the density dips but does not go all the way to zero between the two peaks, as in Fig. 3.2. This is indicative of molecular delocalization, as well as of the possibility of significant quantum mechanical exchanges and ensuing superfluidity. In this respect, the density profile of 32 p-H_2 molecules in the Cs cavity is closer to that of a free p-H_2 cluster comprising the same number of molecules (also shown in Fig. 3.3, dotted line, computed separately in this work), than to that predicted in the stronger glass enclosure. The profile of a free standing cluster extends further out as no repulsive cavity wall is present.

3.A.3   Enhanced superfluid response in cesium cavity

The most important result of this study, however, is that the superfluid response of the cluster which is enclosed in the Cs cavity is greatly enhanced compared to the free ones. For example, in the case of the minimum filling in the Cesium cavity, at $T = 1$ K, corresponding to 32 p-H_2 molecules, the superfluidity of the cluster in the Cs cavity is close to 50%, whereas that of the free cluster at the same temperature is essentially zero (statistical noise level) [55]. In other words, *confinement has the effect of greatly enhancing the superfluid response of the p-H_2 cluster*. This is confirmed by the occurence of exchange cycles including as many as 25 of the 32 molecules in the Cs cavity enclosed cluster, whereas no cycles comprising more than six molecules are observed in a free cluster. The radial density profile of the free cluster displays considerably more structure in the inner shell, suggesting that molecules are more localized than inside the cavity. Indeed, in the case of 30 p-H_2 molecules, the cluster is 100% superfluid when enclosed in a Cs cavity of radius 10 Å, while
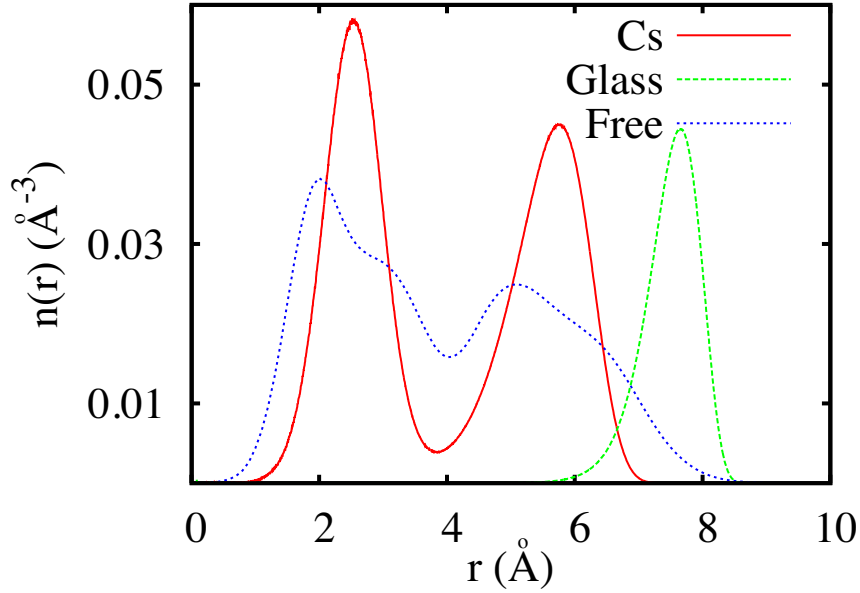
29
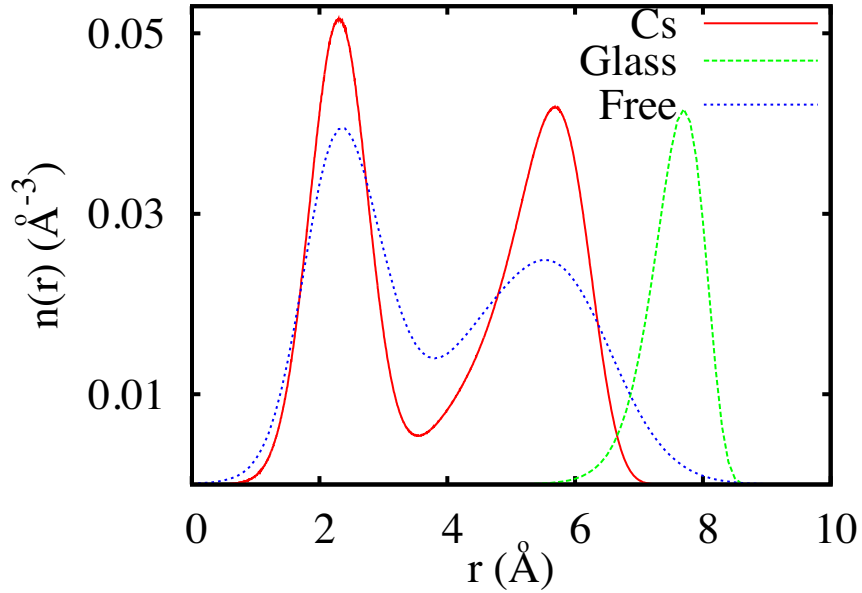
Figure 3.4: Radial density profile $n(r)$ in (Å^{-3}) for 30 p-H_2 molecules inside a Cs cavity (solid line) at $T = 0.5$ K, modeled as explained in the text. Also shown are the profiles for the same number of molecules inside a glass cavity (dashed line) and in a free standing p-H_2 cluster (dotted line). Statistical errors are not visible on the scale of the figure.

the free standing cluster is only 30% superfluid, both at $T = 0.5$ K. Alongside our direct computation of the superfluidity of these clusters in both cases, the radial density profile, Fig. 3.4, and observation of the exchange cycles do lend further evidence to the enhancement of the superfluid response. Fig. 3.5 is a quantitative comparison of the probability of occurrence of permutation cycles including n molecules $(1 \leq n \leq 30)$ in a cluster of 30 p-H_2 molecules enclosed in the Cs cavity, versus in one that is free standing. Indeed, the occurrence of cycles including as many as twenty-five of the thirty molecules is orders of magnitude more likely in a cluster that is enclosed in the Cs cavity [56].
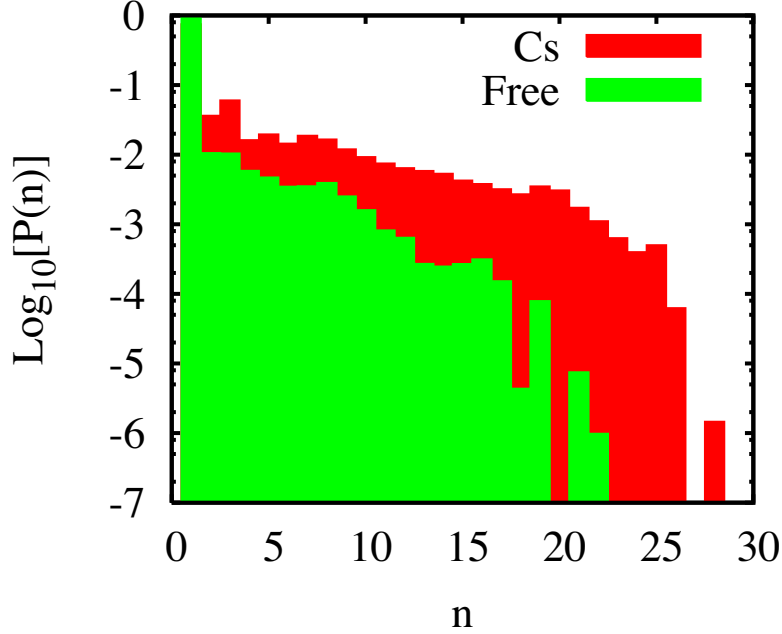
Figure 3.5: Logarithm of the probability of occurrence of permutation cycles of length n (i.e., comprising n p-H$_2$ molecules) in a cluster of thirty molecules enclosed in a Cs cavity (see text), and in a free cluster, at $T = 0.5$ K. Values lower than $\sim 10^{-4}$ should be regarded as statistical noise.

If the cavity is made much more attractive, as is the case for the glass one, exchanges are strongly suppressed, as molecules arrange orderly, to form a thin shell near the surface; on the other hand, in a weakly attractive cavity, confinement renders the cluster more compact than in free space, increasing the tendency of molecules to exchange. Thus, the environment experienced by molecules inside the weak Cs cavity is such that the formation of a solid-like cluster, which takes place in free space, is frustrated; the cluster remains liquid-like, as the substrate is not attractive enough to promote crystallization near the surface, which is what happens in strong adsorbents like silica or carbon.

31

Thus, the main physical conclusion of this work, besides offering a simple explanation for the failure to observe a superfluid response in porous glass, is that it is possible to enhance significantly the superfluid behaviour of p-H$_2$ in certain types of confinement. In principle the theoretical prediction presented in this chapter can be tested against experiment, by measuring the momentum distribution, as explained in Ref. [34], which can provide indirect evidence of the onset of superfluidity in the cavities, assuming that it be experimentally feasible to fashion a matrix consisting primarily of quasi-spherical cavities of radius of order 1 nm, with walls featuring the required attractive properties. However, the ultimate goal of this research effort remains that of identifying the conditions for the possible occurrence of superflow with transport of matter in space.

The results of this investigation suggest that a similar enhancement of the superfluid response might take place inside a cylindrical geometry, if the properties of the substrate are comparable to those that yield the enhancement in spherical confinement. Upon stabilizing a quasi-one-dimensional Luttinger superfluid, then it might be feasible to achieve three-dimensional superflow through an interconnected network of channels, according to a theoretical scenario come to be known as "Shevchenko state" [37]. Such a scenario requires, however, that a strong superfluid response exist in the single channel, and that is the subject of the main research project undertaken in my doctoral research.

Chapter 4

QUASI-ONE-DIMENSIONAL PARAHYDROGEN IN NANOPORES

This chapter presents the results of the major research project carried out in my doctoral work, namely the study of the low temperature physics of parahydrogen confined in nanosized cylindrical channels. As mentioned earlier, this study is in sequel to the observed enhancement of the superfluid response of p-H_2 in spherical confinement and the idea is to see if it is feasible to extend that result to the possibility of achieving bulk superfluidity in 3D porous medium (*Shevchenko* state) comprised of individual spherical cavities interconnected by narrow cylindrical channels (schematically illustrated in Fig. 4.1), in which the physics of p-H_2 closely approaches the one-dimensional limit [36, 57]. The appearance of a global three-dimensional superfluid response crucially hinges on the existence of a quasi-superfluid phase in the single channel, and that is the scenario investigated here.

It is important to note that such a scenario is conceptually *distinct* from that studied in previous works [58], namely weakly interacting quasi-one dimensional channels, e.g., consisting of helium adsorbed in a bundle of carbon nanotubes. What is being studied here is a network of Luttinger liquids that are essentially disconnected, i.e., particles only interact with particles in the same channel only; for, the interaction between particles in different channels is rendered negligible by the average distance, as well as the presence of the medium itself, filling the space between channels. This is nothing like what one has in a bundle of carbon nanotubes, for instance, wherein helium atoms in different quasi-1D channels interact weakly but still appreciably, underlying low temperature phase transitions between 3D and quasi-1D physics. Moreover, helium is a (Luttinger) superfluid in 1D at equilibrium, which is why one can have a three-dimensional superfluid in that way (whereas p-H_2 could not turn superfluid in that setting, precisely because it is not a Luttinger superfluid in 1D).
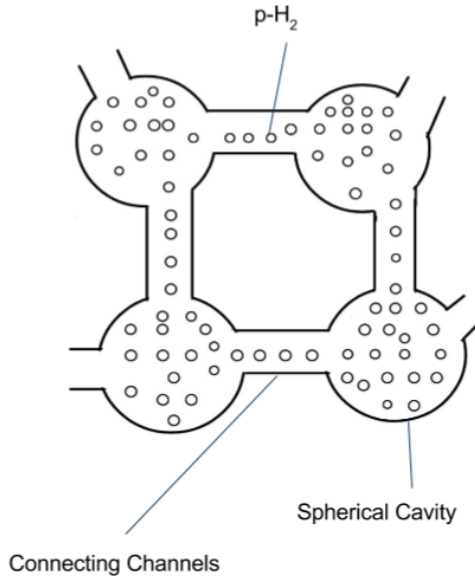
Figure 4.1: Porous medium model: Interconnected spherical cavities.

4.A   Model

The quantum-mechanical model Hamiltonian is expressed in the general form given by Eq. (2.1), which now is aimed at describing a fluid of p-H$_2$ molecules confined inside a cylindrical channel of diameter d and length L, whose axis is in the z direction (the only one along which periodic boundary conditions are relevant). The interaction potential between two p-H$_2$ molecules utilized in here is the revised version of the Moraldi pair potential [46] also used in the study of Chapter 3. It is worth repeating that the aim of using such a potential is that of obtaining a quantitatively more accurate description of the equation of state of p-H$_2$ at high pressure. This is particularly important in the vicinity of the surface of the channel, where the pressure could conceivably exceed significantly that in the middle of the channel.

For the the interaction V between a p-H$_2$ molecule and the wall, we made use of the expression arising from the integration of a Lennard-Jones potential over an infinite continuous medium surrounding the cylinder, regarded as infinitely long [59]. The resulting expression only depends on the radial distance of a molecule from the axis of the cylinder, and contains two parameters: *a)* a characteristic length a, which is essentially the distance of closest approach of a molecule to the wall of the channel, where the potential becomes strongly repulsive, and *b)* an energy D, which is basically the depth of the attractive well of the potential which particles experience from the wall [60]. These two parameters are adjusted to reproduce, as accurately as allowed by such a relatively simple model, the interaction of a particle with a substrate.

The values of the parameters of the potential utilized in this work are reported in Table 4.1. They were taken from Ref. [61], except those for glass,

Substrate	D (K)	a (Å)
Cs	37.8	3.88
Rb	39.7	3.87
K	44.4	3.76
Na	69.5	3.40
Li	99.7	3.19
Mg	191.8	2.76
Glass	232	2.22

Table 4.1: Potential parameters D and a utilized in this work. The values are taken from Ref. [61]. Substrates are listed in order of increasing strength, from top to bottom.

which were obtained starting from those proposed in Ref. [62] for helium atoms near a glass substrate, using Lorentz-Berthelot mixing rule to adjust them for p-H_2. The resulting potentials are shown in Fig. 4.2.
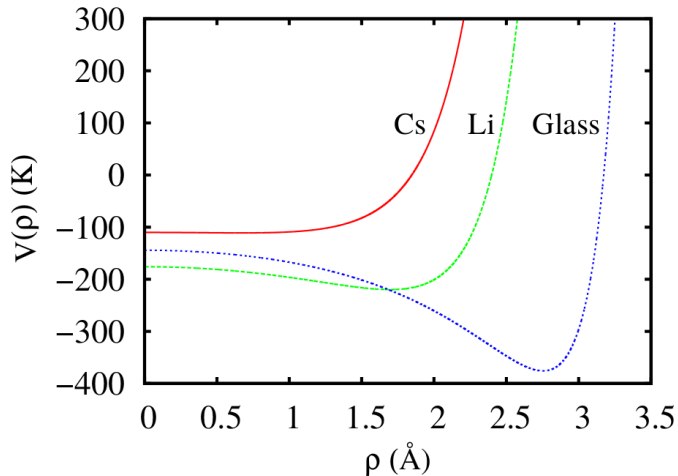
Figure 4.2: Potentials describing the interaction between a p-H_2 molecule and the wall of the confining cylindrical channel, for some of the substrates considered here. Cs (cesium) is the weakest, glass is the most strongly attractive, and Li (lithium) has intermediate strength. Here, ρ is the distance of a particle from the axis of the channel.

The focus here is mostly on metallic alkali substrates which are known to be weak adsorbers, for the purpose of identifying physical conditions in which the equilibrium phase of the system may be a quasi-1D liquid, i.e., with p-H_2

molecules lined up along the axis of the channel, as opposed to concentric, solidlike shells which are expected to form inside a strong adsorber like silica.

The above model, similar to that utilized in the study of p-H_2 inside spherical cavities (described in the previous chapter), clearly contains major simplifications, notably the assumption that the interactions between two p-H_2 molecules can still be regarded as central, when in fact it is quite plausible that such an interaction may be significantly altered in the presence of a strong attractive wall, which could have the effect of polarizing molecules. Moreover, the cylindrical cavity wall itself is regarded as smooth, free of corrugation or defects. These simplifications can in part be justified by the fact that the substrates of interest are weak, and therefore the distance from the surface (over 3 Å) at which molecules should be sitting (this is confirmed by our results) is such that the influence of the substrate on the intermolecular interaction ought to be relatively minor. The same argument justifies the neglect of surface defects and corrugation, an assumption routinely made in numerical studies of adsorption of He or p-H_2 on alkali substrates [63]. And despite its simplicity, such a model allows us to address the physical question that we wish to pose here, namely the effect of confinement on the superfluid response of p-H_2. Equivalent, or even simpler models (e.g., cavities with hard walls) have been utilized to study structure of ^{4}He in confinement [36, 57, 58].

4.A.1   Luttinger Liquid Theory

As the diameter of the channel is reduced to one nm or less, which is the physical setting of interest here, the physics of a fluid confined in it approaches the one-dimensional limit, and becomes therefore amenable to interpretation

within the framework of Luttinger liquid theory [35] as shown, for example, by computer simulation of ^{4}He confined in nanopores of such a characteristic size [36, 57]. The LLT provides an elegant and universal description of Bose or Fermi systems in one dimension, in terms of linear quantum hydrodynamics. It asserts that, while no true long range order exists in 1D, two-particle correlations display a slow power-law decay as a function of interparticle separation r. The specific power law, in turn, reflects different physical properties of the underlying system. Consider for definiteness the pair correlation function $g(r)$, measuring the relative probability that any two system particles be at any given time at a distance r from one another. The LLT asserts that at any finite temperature T will take on the following behavior in the thermodynamic limit:

$$g(r) \sim 1 - \frac{1}{2\pi^2 K n^2 r^2} + A \cos(2\pi n r)\frac{1}{n^2 r^{2/K}} \tag{4.1}$$

Here, n is the linear density of particles and A a non-universal, system-dependent constant. The Luttinger parameter K describes how quickly the oscillations of $g(r)$ decay at long distance; based on its value one can meaningfully differentiate between phases that are "quasi-crystalline" or "quasi-superfluid" in character. Specifically, if $K > 2$ the static structure factor will develop peaks (experimentally indistinguishable from conventional Bragg peaks) at reciprocal lattice vectors, which is the experimental signature of a crystalline solid. On the other hand, if $K < 0.5$ the system features a robust propensity to superflow, and for $0.5 \leq K \leq 1.5$, the system can be regarded as a "glassy" insulator (at the high end of the interval), or as a weak superfluid, subjected to pinning by either disorder or an external potential. Henceforth, whenever speaking of "crystal" versus "superfluid", we shall refer to the above

classification.

The scenario that we are exploring here, namely that of three-dimensional superflow through a network of quasi-one-dimensional, interconnected channels, known as "Shevchenko state" [37, 38], requires that the system be a Luttinger superfluid in the individual channels; that is the conjecture that has been investigated in this work, by means of computer simulations. Now, in one mathematical dimension, the ground state of condensed p-H_2 is known to be a Luttinger insulator, with a value of the parameter $K \approx 3.5$ at the equilibrium density, growing monotonically as the system is compressed. Thus, one may wonder how such a state of affairs, which rules out the Shevchenko scenario for the reason mentioned above, might change if the system approaches the one-dimensional limit in the tight confines considered here. Should one not expect the value of K in confinement to approach that in one dimension?
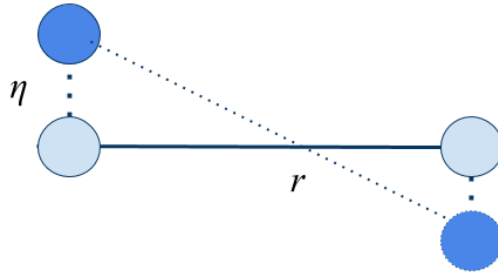
Figure 4.3: Schematic representation of the physical origin of the softening of the intermolecular potential due to zero point motion in the transverse direction.

One may qualitatively understand how a reduction of the value of the parameter K may occur, as a result of molecular quantum zero point motion in the direction perpendicular to the axis of the cylinder (transverse direction), along which molecules line up at low linear density, if the substrate is sufficiently weak; Fig. 4.3 shows this effect schematically. Consider two molecules

at an *axial* distance r; because they execute quantum oscillations in the transverse direction, the effective potential $\tilde{v}(r)$ describing the interaction between them includes contributions from the value of the "bare" potential $v(r)$ at distances that are *greater* than r. The overall effect is that of softening the potential, in particular rendering it less attractive, which in turn can be expected to reduce the propensity of the system to crystallize. One can easily obtain a semi-quantitative estimate of the effect by modeling molecular transverse motion by means of a simple harmonic approximation [64], characterized by a root-mean-square transverse displacement η, and obtain $\tilde{v}(r)$ by means of the following straightforward integration:

$$\tilde{v}(r) = \int_{-\infty}^{+\infty} dz \; dz' \; \psi^2(z) \; \psi^2(z') \; v(\sqrt{r^2 + (z-z')^2}) \qquad (4.2)$$

with $\psi^2(z) = A \, \exp[-z^2/2\eta^2]$, A being a normalization constant. The effective inteparticle potential that results is shown in Fig. 4.4, assuming a Lennard-Jones interaction for $v(r)$ and for various values of η ($\eta = 0$ obviously corresponds to $\tilde{v}(r) = v(r)$).

4.B   Simulations

In this section, some technical details of the calculations are furnished. Most of the simulations carried out in this work, using the methodology described in Chapter 2, pertain to a system with diameter d=10 Å, but some for a narrower (wider) channel of diameter d=5 Å (d=20 Å) were performed as well. The value of L, i.e., the length of the cylindrical channel utilized in most of the calculations is 160 Å, which was empirically established to be
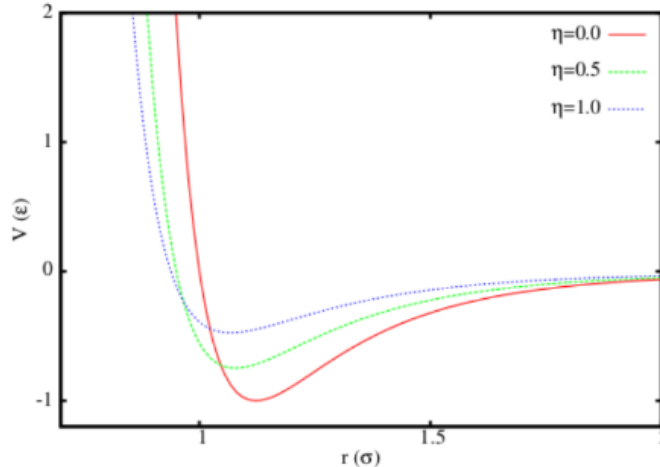
Figure 4.4: Effective one-dimensional potential between two particles which can execute small transverse excursions, modeled as explained in the text. The bare potential $v(r)$ is assumed to be a Lennard-Jones one, and so distances and energies are expressed in terms of the parameters σ and ε.

sufficient to capture quantitatively the physical behaviour inside an infinitely long channel. This results in a typical number of particles of the order of a few hundred for most simulations, 600 being the largest.

In this study, like in that described in Chapter 3, instead of making use of the simple imaginary-time discretization of the Euclidean action described in Chapter 2 (Eq. 2.8), a more accurate one was adopted (specifically, accurate to fourth order [48] in the imaginary time step τ, as opposed to the second order accuracy in τ afforded by Eq. 2.8). Simulations carried out for a few cogent cases yielded results showing that the values of the physical averages obtained with a time step $\tau_{\circ} = 1/640$ K^{-1} are indistinguishable from those extrapolated to the $\tau \to 0$ limit, within statistical uncertainties. Thus, most of the results presented here correspond to simulations with $\tau = \tau_{\circ}$.

4.C Results

Most of the results presented and discussed here pertain to adsorption of a p-H_2 fluid inside a cylindrical channel of diameter d=10 Å; the physical behaviour observed inside channels of greater or smaller diameter will be dealt with at the end.

We begin by discussing the energetics. Fig. 4.5 shows computed values of the energy e per p-H_2 molecule as a function of the linear particle density $\nu = N/L$, for three of the alkali substrates considered here. The results shown here are for a temperature T=1 K; energy estimates for this system, as well as structural properties, have been consistently found not to change significantly below $T = 4$ K, at all physical conditions explored in this work. Thus, the results can be regarded as ground state (T=0) values.
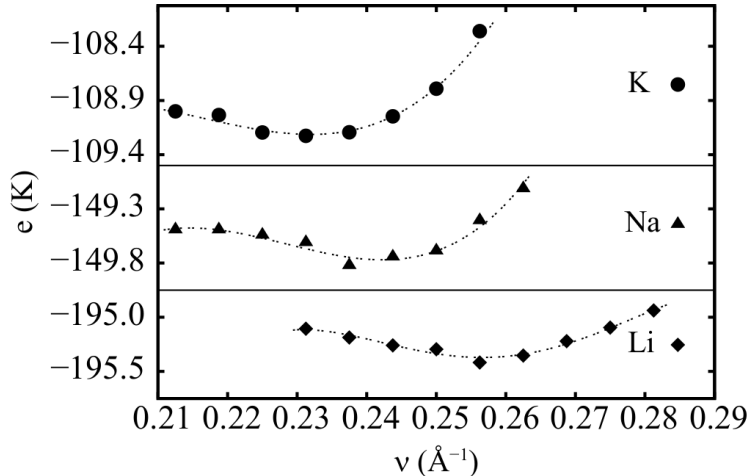
Figure 4.5: Energy per p-H_2 molecule e (in K) versus linear density ν (in Å^{-1}), at $T = 1$ K, inside a cylindrical channel of diameter d=10 Å. Results are shown for three different substrates, namely K (filled circles), Na (filled triangles) and Li (diamonds), listed in order of increasing strength (see Table 4.1). Dashed lines are polynomial fits to the data. Statistical uncertainties are of the order of the symbol size.

The curves all display a minimum at the equilibrium density, corresponding

Figure 4.6: Three-dimensional density of p-H_2 inside a cylindrical channel of diameter d=10 Å, plotted as a function of the distance from the axis. Curves pertain to different substrates, at the corresponding equilibrium densities. Statistical errors are not visible on the scale of the figure.

to energy values all well below the bulk chemical potential of p-H_2, namely -90 K. It is noteworthy that a stable adsorbate also exists inside a Cs channel (the energy minimum in that case is -95 K), which is in contrast to the case of an infinite flat Cs substrate, which is actually not wetted by p-H_2 [63]. Thus, the cylindrical geometry confers to the substrate greater adorption strength. It is seen that the equilibrium density increases with the strength of substrate adsorption, from a value close to 0.23 Å^{-1} for a K substrate (on a Cs it is essentially the same), which is $\sim 5\%$ higher than the corresponding value for the purely 1D system [19], to as high as 0.255 Å^{-1} inside a Li channel. Despite the increased equilibrium density of quasi-1D p-H_2 confined in alkali metals, it turns out that the propensity of the system to crystallize is reduced, compared to pure 1D. This is as a result of the softening of the intermolecular potential, which arises from the molecular zero-point motion in the transverse direction as explained above. The adsorbate in these subtrates displays a quasi-1D

character, as shown by the p-H_2 density profiles, computed with respect to the axis of the channel (Fig. 4.6).
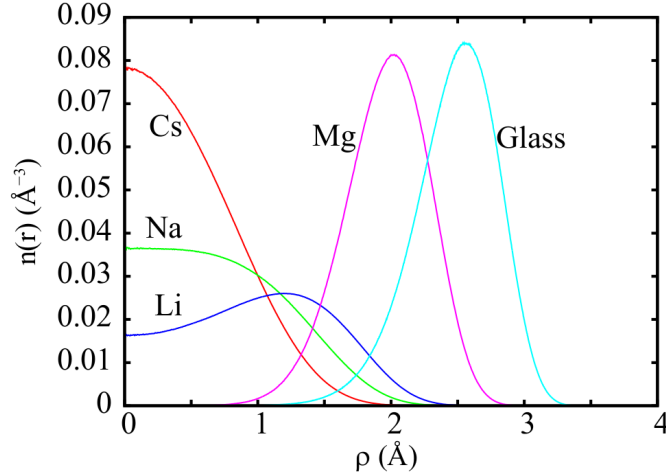
Fig. 4.6 shows the three dimensional density of p-H_2 inside a cylindrical channel of diameter $d = 10$ Å, plotted as a function of the distance from the axis at equilibrium density in each of the substrates. On the two least attractive substrates among the five shown (Cs and Na), molecules line up along the axis of the cylinder, the greater pull that they experience in the case of a Na substrate resulting in a greater spread of the molecular wave function in the transverse direction. At the opposite end, on the stronger substrates such as Mg and glass, the density of p-H_2 is negligible on the axis, as the equilibrium phase consists of a single cylindrical shell coating the wall, with molecules sitting at a closer distance from it in the case of glass.

The physics of the system on the substrate labeled as Li, on the other hand, in a way interpolates between strong and weak adsorption [65]. The density profile displays a maximum off the axis, but the density on the axis itself remains finite. This suggests that molecules arrange on a helix, winding around the axis; this structure remains largely 1D in character.

We now tackle the most interesting issue, namely the physical effect of the significant molecular excursions away from the axis of the channel, on the physical character of the quasi-1D adsorbates. As mentioned above, one may expect such excursions to soften the intermolecular interaction, responsible for the strong propensity of the system to crystallize, possibly with the result of imparting to the system quasi-superfluid behaviour. In order to address this issue, we study the reduced pair correlation function $g(r)$, where r is the component of the distance between two particles along the axis of the channel. For systems that approach the 1D limit (and in our study that

44
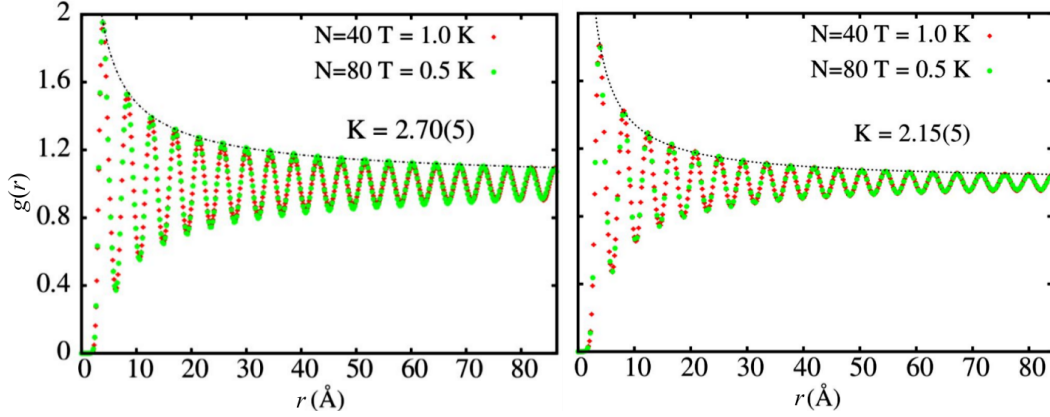
Figure 4.7: Pair correlation functions for p-H_2 confined in a cylindrical channel of diameter d=10 Å. Left panel shows results for a Cs substrate, right panel for a Na one. In both cases results are shown for the two temperatures T=1 K, for a system of $N = 40$ molecules, and T=0.5 K, for a system comprising $N = 80$ molecules. Statistical errors are smaller of the sizes of the symbols. Dashed lines represent fits to the maxima of $g(r)$ as explained in the text.

means equilibrium p-H_2 layers adsorbed inside channels whose walls have the adsorption properties of the alkali metals in Table 4.1), the $g(r)$ is expected a) to depend only on the product LT in the limit $L \to \infty, T \to 0$, and b) to conform to the behaviour predicted by Eq. 4.1, allowing one to infer [19, 36] the value of the Luttinger parameter K for the particular system of interest.

Fig. 4.7 shows pair correlation functions computed for p-H_2 inside a Cs (left) and a Na (right) channel, in both cases for two different temperatures, namely $T = 0.5$ and 1 K, and two different system sizes, comprising $N = 40$ and 80 molecules. In both cases, calculations are carried out at the equilibrium density, which, as mentioned above, is slightly above that in purely 1D. As one can see, collapse of the data is clearly observed. The value of the parameter K can be obtained by fitting the computed $g(r)$ to the expression (4.1) or, somewhat more simply, its maxima to the expression $f(r) = 1 + A/r^{2/K}$.

For the weakest substrate, for which the adsorbate is closest to the 1D

45

limit, i.e. for which molecular excursions in the transverse direction are most limited, the determined value of K is 2.70(5), appreciably lower than that for a purely 1D system (3.5). As the adsorption strength of the wall of the channel increases, our estimate of K gradually decreases, the lowest value (very close to 2) attained for a Li substrate.

As shown above (Fig. 4.6), if the wall of the channel is taken to be slightly more attractive than Li (i.e., Mg), then the equilibrium phase is a concentric cylindrical shell, with essentially no molecules in the central part of the channel. The effective 2D coverage of such a layer can be inferred from the data shown in Fig. 4.6, and is ~ 0.067 Å^{-2}, i.e., the same with the equilibrium coverage [18] of p-H$_2$ in 2D at $T=0$. Actually, the physics of such an adlayer is quite close to that of 2D p-H$_2$; that is, the system displays solidlike behaviour, with molecules localized in space, quantum-mechanical exchanges are virtually absent and, consequently, no trace of superfluidity can be observed. On increasing the density, a second, quasi-1D inner layer eventually forms; we studied this system for the case of a glass channel. For simplicity, we utilized in these calculations an effective harmonic potential, adjusted to reproduce, in the vicinity of the axis of the cylinder, the combined effect of the interaction of the molecules with the wall of the channel, as well as with the molecules in the shell coating it. The resulting, fairly tight confining effect for the molecules in the central region, combined with the relatively high linear density of thermodynamically stable inner layers, imparts to the system in the inner part a markedly solidlike behaviour. Indeed, characteristic values of the parameter K for quasi-1D inner p-H$_2$ layers surrounded by a p-H$_2$ cylindrical shell are generally ≥ 3.5.

We now comment on the results obtained in narrower and wider channels.

Inside a channel of diameter d=5 Å, no adsorption occurs except for the most attractive of the substrates considered here, namely glass. The quasi-1D inner layer closely approaches the physics of 1D p-H$_2$, with essentially the same value of the linear equilibrium density and Luttinger parameter K. Inside a channel of wider diameter (d=20 Å), on the other hand, adsorption occurs for all substrates except Cs, and the equilibrium phase is again a single, solidlike cylindrical shell, concentric with the wall and with an equilibrium density close to that of 2D p-H$_2$.

4.D   Summary

The extensive simulation studies performed in this work for a realistic model of p-H$_2$ adsorbed in the interior of a cylindrical channel of diameter ranging from 5 to 20 Å yield evidence that, although confinement can somewhat reduce the strong tendency of the system to crystallize, as observed in spherical cavities, nevertheless the effect is quantitatively more limited in a cylindrical geometry. Specifically, if the diameter of the channel is as large as merely 2 nm, then the physics observed is qualitatively very similar to that which takes place when p-H$_2$ is adsorbed on a flat substrate [63]. On the other hand, inside narrow channels of diameter less than 1 nm, p-H$_2$ will form quasi-one-dimensional adsorbates (if the substrate is sufficiently strong) that closely reproduce the physics of the system in purely one dimension, i.e., the phase is crystalline in nature (in the Luttinger sense). A cylindrical channel of diameter close to 1 nm, with a substrate that is relatively weak (e.g., Li) provides a confining environment in which the interplay of reduced dimensionality and quantum excursions off the axis can lead to different physics, specifically to the

stabilization of quasi-one-dimensional phases with a much reduced tendency to crystallize. This is qualitatively consistent with the enhancement of the superfluid response of p-H_2 clusters trapped inside a spherical cavity; however, the effect is quantitatively far less significant in the quasi-one-dimensional geometry considered in this work, as the predicted reduction of the Luttinger parameter K from its value in one dimension (3.5) all the way to approximately 2 does not entail a fundamental change of the physical character of the system, which remains well in the insulating sector of the LLT. Consequently, any scheme aimed at stabilizing a bulk superfluid phase of p-H_2 in a network of interconnected cavities seems to face the insurmountable hurdle that no superflow may be sustained inside narrow cylindrical channels connecting two adjacent cavities. Thus, this study seems to rule out definitively such a scenario.

Chapter 5

INVESTIGATION OF THE METASTABLE FLUID PHASE OF PARAHYDROGEN

It has been shown in the preceding chapters that the propensity of p-H$_2$ to crystallize at low temperature can be somewhat reduced in confinement. However, the scenario of a bulk superfluid phase of p-H$_2$ in a networked porous medium does not appear feasible, as no quasi-one-dimensional superfluid phase can be stabilized. At this time, no other credible avenue seems to exist, and the putative superfluid phase of p-H$_2$ remains therefore elusive. In particular, no approach based on confinement, or reduction of dimensionality, seems likely to succeed.

The question of whether a hypothetical metastable fluid phase of p-H$_2$ *would* undergo a superfluid transition remains open, however. As mentioned in the Introduction, there exists a theoretical estimate of the transition temperature, placing it in the vicinity of 2 K, but such a prediction has not been

corroborated by robust first principle calculations, based on realistic microscopic potentials.

This issue has so far not been addressed by simulation, owing to the intrinsic difficulty to prevent even a simulated system of relatively small size (i.e., ~ 100 particles) from spontaneously crystallizing. Indeed, a common misconception among nonpractitioners of computer simulations, is that one will not observe spontaneous freezing on a computer, unless particles are placed at specific lattice sites at the start of the run. This contention can be easily disproven by carrying out the simple "computer experiment" described below.

5.A   Computer experiment I

A simulation of N=128 p-H_2 molecules at a temperature T=1 K is carried out, using the methodology illustrated in Chapter 2. Particles are enclosed in a cubic box, the density set at 0.023 Å^{-3}, namely the freezing density of liquid p-H_2 at T=13.8 K. The interparticle potential is chosen initially to be the Lennard-Jones one; however, while the well depth ε is set to its recommended [43] value of 34.16 K, the hard core length σ is taken to be 2.556 Å, i.e., the same as that of the Lennard-Jones potential describing the interaction between two He atoms, which is significantly smaller than the standard value for p-H_2 (2.96 Å). The resulting potential, while it has the same well depth, is substantially "softer" than the ordinary Lennard-Jones potential for p-H_2, allowing molecules to come to a considerably closer distance than they do in actual p-H_2.

Although particles are initially arranged on a (simple cubic) lattice, the simulated system melts rapidly, and a robust superfluid response sets in. In-
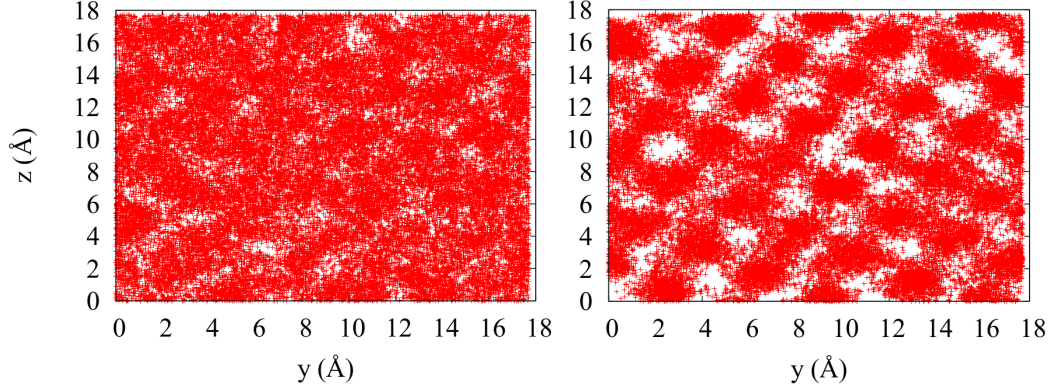
Figure 5.1: Instantaneous "snapshots" of many-particle configurations (particle world lines) generated in the course of a simulation of a system of N=128 p-H$_2$ molecules at a density 0.023 Å^{-3}. The temperature is $T = 1$ K. The view is along the x direction. In the configuration shown in the left panel particles interact via a Lennard-Jones potential with ε=34.16 K and σ=2.556 Å. The configuration shown in the right panel is obtained by restarting the simulation of left panel, but with particles now interacting via the Silvera-Goldman potential for p-H$_2$.

deed, long permutation exchanges quickly appear, and the system is 100 % superfluid [67]. The left panel of Fig. 5.1 shows a many-particle configuration (particle world lines) generated in the course of the simulation described (the view is along the x direction). There is no evidence of any kind of order, particle density is essentially uniform and particle paths overlap, consistently with the frequent occurrence of exchanges. As a result, it is impossible to identify visually individual particles.

The second part of the experiment consists of restarting the simulation from the last configuration generated in the previous run, but with the interaction potential now switched to the Silvera-Goldman, i.e., a realistic potential for p-H$_2$. Right panel shows a configuration generated in the simulation restarted as explained. The physical scenario is clearly very different, as particles are now arranged on a regular lattice. Such an arrangement emerges without any

51

intervention on the part of the investigator, witness the fact that the lattice is tilted at a random angle with respect to the axes of the simulation cell. Long exchange cycles of p-H_2 molecules present in the initial configuration quickly disentangle, particles re-acquire their identity, and can now be easily distinguished. Concurrently, the superfluid signal drops to zero.

It is noteworthy that a similar experiment carried out on ^{4}He slightly above the freezing pressure, when the equilibrium configuration is a crystal, shows much greater resilience of the overpressurized, metastable superfluid phase, in which the simulated system is "locked" by persistent long exchanges [66]. All of this points to the very different physical character of these two condensed matter systems, p-H_2 being much closer in its behaviour to a classical system. It also underscores the difficulty of investigating by simulation a metastable fluid phase of p-H_2, rendered problematic by the strong tendency of the system to solidify. This problem can be alleviated by studying systems of bigger sizes, for which the free energy barrier required to "jump" from the metastable to the stable phase (an extensive quantity) can become large enough that the system may be locked in the former – for a sufficiently long time that one may collect useful statistics. Large system sizes, however, have become accessible to quantum simulations only in relatively recent times.

The above results also show how it is not just the well depth that causes crystallization, but rather the combination of well depth and size of the hard core radius. This can be expressed more generally and quantitatively in terms of the so-called De Boer's parameter.

5.A.1   De Boer's parameter

Consider a generic Bose system, and for simplicity let us assume that particles have spin zero. We are assuming a Lennard-Jones type interaction, and express the many-body Hamiltonian in dimensionless units as follows:

$$\hat{h} = -\frac{1}{2}\,\eta\,\sum_{i=1}^{N} \tilde{\nabla}_i^2 + 4\sum_{i<j}\left[\left(\frac{1}{r}\right)^{12} - \left(\frac{1}{r}\right)^{6}\right], \qquad (5.1)$$

having introduced the *De Boer's parameter* $\eta = \hbar^2/(m\varepsilon\sigma^2)$. η is the single parameter that determines the physical character of the system in the ground state. In particular, if $\eta \to 0$, quantum-mechanical effects are increasingly unimportant, and the behaviour of the system is nearly classical; consequently, its ground state is a crystal, as predicted by classical mechanics, as the arrangement of particles on a crystal lattice is that which minimizes the potential energy. On the other hand, if η is appreciably different from zero one may expect quantum-mechanical effects to be important, possibly leading to a substantial modification of the classical predictions, not only in quantitative but also qualitative terms (e.g., the ground state being a liquid, as is the case for He).

Fig. 5.2 shows the $T=0$ equation of state for various values of the quantum parameter η. Here, ρ is the three-dimensional density of particles, in units of σ^{-3}, while $e(\rho)$ is the energy per particle, in units of ε. These equations of state were obtained by computing the energy per particle as a function of the density and extrapolating the results to $T=0$, using the methodology described in Chapter 2. It was generally found that the results obtained at a reduced temperature of $T = 0.05\,\varepsilon$ are indistinguishable from those extrapolated to $T = 0$, within statistical uncertainties. These calculations were carried out on systems
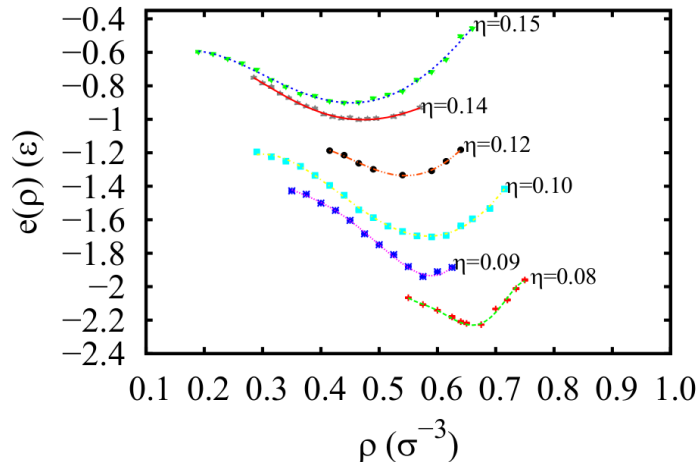
Figure 5.2: $T \to 0$ equation of state ($e(\rho)$ curve) for Lennard-Jones Bose systems, for various values of η. Here, ρ is the three-dimensional density of particles and, the energy per particle is expressed in units of ε. The statistical uncertainties on the computed energies are of the order of, or less than, the size of the symbols. Thread lines are polynomial fits to the data.

comprising typically $N{=}128$ particles. The contribution to the total energy from the particles lying outside the main simulation cell is estimated by radially integrating the attractive tail of the potential energy from the boundary of the simulation cell to infinity while approximating the (three-dimensional) pair correlation function, $g(r)$, as 1 according to standard procedure [41]. This contribution usually amounts to less than $\lesssim 1\%$ of the total potential energy of the system. The results shown in Fig. 5.2 are in good quantitative agreement with the variational theory of Nosanow and collaborators [68, 69].

As the value of η increases, the equilibrium density ρ_e (corresponding to the minimum of the curve) shifts to lower values; the ground state of the system is a superfluid liquid for $\eta \gtrsim 0.15$, a crystal for lower values. The value of η for p-H_2 is 0.08, placing it well into the crystalline sector; on the other hand, for ^{4}He it is $\eta = 0.18$, consistently with its ground state being a superfluid. An interesting question that can be asked is whether it is possible for a system

whose ground state is crystalline to be *stretched* [70] (i.e., at negative pressure) into a metastable, low density superfluid. The region of density within which this is physically allowed is $\rho_S \leq \rho \leq \rho_e$, where ρ_S is known as the *spinodal density*, and is defined by the condition $d^2e/d\rho^2 = 0$ (i.e., change of convexity of the $e(\rho)$ curve).

As mentioned previously, $\eta = 0.08$ corresponds to p-H$_2$. The equilibrium density in this case is estimated in this work to be $\rho_e \sim 0.68\ \sigma^{-3}$, which corresponds to ~ 0.026 Å^{-3}, in excellent agreement with the experimentally determined equilibrium density of p-H$_2$ in the $T \to 0$ limit [71]. This system is a crystal at equilibrium and remains such (i.e., non-superfluid) all the way to the spinodal density. This means that, in analogy with what is already established in one and two dimensions [18, 19], at sufficiently low temperature no metastable fluid phase of p-H$_2$ exists. Although this result strictly applies in the $T \to 0$ limit, it clearly represents another potentially serious hurdle to overcome in the quest for a metastable superfluid phase of p-H$_2$, as no reliable estimate presently exists of the superfluid transition temperature [72].

It is worth mentioning, to conclude this section, that the simulations carried out here cannot furnish a definitive answer as to whether there exists a specific value of η for which the ground state of the system is a crystal, but a metastable superfluid phase exists at negative pressure; this is due to the difficulty of estimating the location of ρ_S with the required precision. The results presented in Fig. 5.2 only allow one to state that, if such a scenario occurs, it may only be within a relatively narrow range of values of η, specifically in the neighborhood of $\eta \approx 0.13$. While there is no naturally occurring Bose fluid characterized by such a value of η, this issue may be addressed within cold atom physics, owing to the "tunability" of the interparticle interactions [39].

5.B   Computer experiment II

In this section the results are presented of simulations of a metastable phase of fluid p-H_2. The lowest temperature down to which such a phase could be simulated in this work is $T=3$ K, for which the system can be assessed to be in a disordered, liquid-like phase.

The simulations were carried out on a system comprising $N=512$ particles. The system is initially prepared in the desired, metastable liquid phase typically by means of the same procedure described in 5.A, namely by initially setting the interaction to a Lennard-Jones potential with the well depth of p-H_2 but a shorter radius (typically $\sigma=2.556$ Å), allowing the system to relax to a fluid phase and then changing the interaction to one appropriate for p-H_2 [73]. Although, as mentioned in 5.A, given a sufficiently long time the crys-

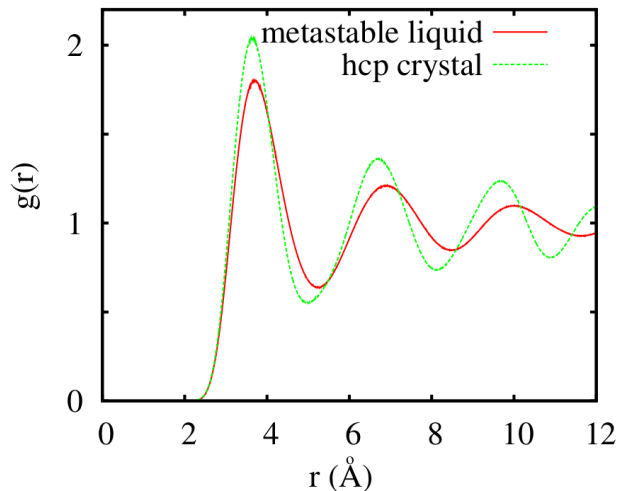
Figure 5.3: Pair correlation function for metastable liquid p-H_2 at density 0.0230 Å^{-3}, computed at temperature $T=6$ K (solid line). Also shown for comparison (dashed line) is the same quantity for the equilibrium crystalline (hcp) phase of p-H_2 at the same temperature, at density 0.0261 Å^{-3}.

talline phase will eventually start nucleating, the idea is that one may be able

to observe the mestable fluid phase for a sufficiently long time to accumulate reliable statistics on its physical properties. Obviously, of particular interest is any quantitative indication of an incipient superfluid transition

Fig. 5.3 shows the computed pair correlation function $g(r)$, which was first introduced in Chapter 4 for the one-dimensional case. The quantity plotted in the figure above is its three-dimensional analogue, normalized as follows:

$$\frac{\int dr \; r^2 \; g(r)}{\int dr \; r^2} = \frac{N-1}{\Omega} \tag{5.2}$$

where Ω is the volume of the simulation cell and N the number of particles. The solid line shows the $g(r)$ for the metastable liquid phase at a temperature $T=6$ K, for a system density equal to the freezing density at $T=13.8$ K, namely 0.023 Å^{-3}. Also shown for comparison (dashed line) is the same quantity computed for the equilibrium crystalline phase (hcp structure) at the same temperature, which corresponds to a density 0.0261 Å^{-3}. The qualitative and quantitative differences are clear; specifically, the $g(r)$ for the solid phase displays much more pronounced oscillations, which persist at greater distances than in the liquid phase. Naturally, the liquid-like nature of the system could be ascertained by visual inspection of the configurations generated in the course of the simulation, none of which suggested any kind of density long-range order.

At this point it is worth mentioning again that the original, crude prediction by Ginzburg and Sobyanin [11], based on a picture of fluid p-H$_2$ as a noninteracting Bose gas, identifies the superfluid transition temperature as that of the onset of Bose-Einstein condensation. For p-H$_2$, that is approximately 6 K, twice as high as that which the same argument provides for ^{4}He, whose atomic

mass is very nearly twice that of a p-H_2 molecule (the difference in the mean interparticle distance between the two systems is less than 2%). Qualitatively, such a temperature is that at which exchanges of indistinguishable particles begin to occur in the noninteracting system, i.e., the thermal wavelength is of the order of the average interparticle distance. Now, for ^{4}He, the estimate obtained in this way is surprisingly close to the actual superfluid transition temperature of 2.18 K [1]; indeed, although interactions lower the transition temperature slightly, atomic exchanges are observed in a PIMC simulation of ^{4}He at T=3 K at saturated vapour pressure, albeit infrequently [74]. Markedly
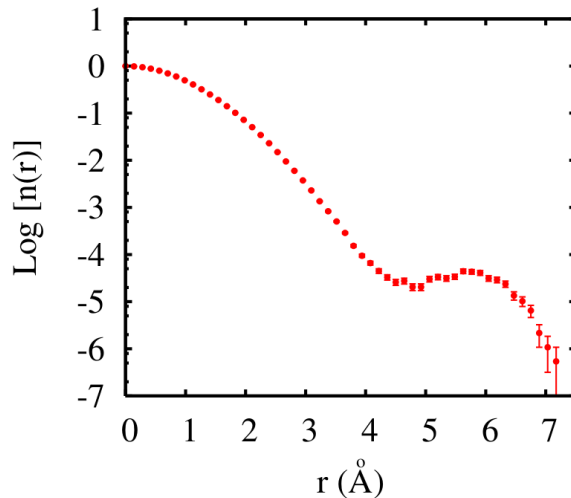
Figure 5.4: One-body density matrix of metastable liquid p-H_2 at density 0.0230 Å^{-3}, computed at temperature T=4 K. The same result for the same quantity, computed at T=6 K and T=3 K is indistinguishable from that shown here, within statistical errors.

different is the situation for p-H_2, as the simulations carried out in this work show. In particular, exchanges are all but absent not only at T=6 K, but even at T=3 K; in other words, even at this relatively low temperature (at least with respect to the original prediction of Ref. [11]) p-H_2 molecules act as if they were *de facto* distinguishable. This is clearly in stark contrast with ^{4}He,

which at T=1.5 K is well in the superfluid phase, with long exchange cycles spanning essentially the whole system. The failure of the system to develop long exchanges has the immediate consequence that no off-diagonal long range order develops, down to the lowest temperature reached in this work; specifically, the one-body density matrix, which in three dimensions must asymptote to a finite value at long distance (the condensate fraction $n_\circ$ [6]), is instead observed to decay exponentially, with no appreciable temperature dependence (Fig. 5.4). This can be again contrasted with the behaviour of the same quantity in liquid ^{4}He (Fig. 5.5), i.e., the value of the one-body density matrix in this case changes by orders of magnitude, going from T=3 K and T=1.5 K, as a consequence of the appearance of long exchanges below the superfluid transition.
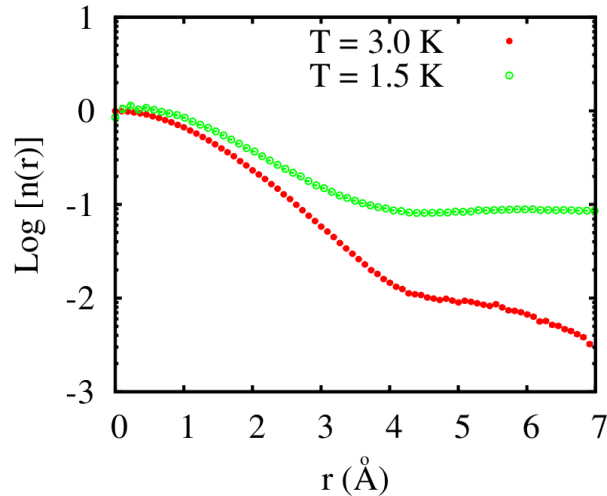

Figure 5.5: One-body density matrix of ^{4}He at equilibrium density, computed at temperature T=3 K (filled symbols), and T=1.5 K (open symbols).

It is important to note that the absence of exchanges in the simulation of the metastable liquid phase of p-H$_2$ can not be attributed to algorithmic or computational inefficiency, as would have been the possibility with a PIMC

implementation as that described, for example, in [8], where the sampling of long permutations is bound to become exponentially inefficient for large system sizes. In this case, the continuous-space Worm Algorithm, described in Chapter 2 was adopted, and in the course of each simulation a large number of "swap" moves [48], quickly leading to long permutation cycles in a superfluid system like ^{4}He, were attempted and accepted. The system does not develop such long cycles for physical, not computational reasons.

The exponential, temperature-independent decay of the one-body density matrix observed here down to $T=3$ K represents a strong piece of numerical evidence to the effect that even the estimate of the superfluid transition temperature obtained by Apenko [13], taking in part interactions into account and revising the original one by Ginzburg and Sobyanin to approximately 2 K, is still at least an order of magnitude too high.

Obviously, based on the conclusion of the previous section, this leaves investigators with the prospects of searching for a metastable superfluid phase of p-H_2 that may exist only in a very narrow range of temperature, before a sufficiently low T is reached where no metastable fluid phase exists, as predicted by the results of the previous section. It is also important to stress that the low temperature at which superfluidity might be possible, perhaps of the order of 0.1 K, is presently out of reach of any known experimental method.

What is the physical reason underlying the radically different behaviour of metastable liquid p-H_2 and liquid ^{4}He? As mentioned above, the mean interparticle distance in the two liquid phases is comparable, of the order of 3.51 Å in p-H_2 and 3.58 Å in ^{4}He. On the other hand, the radius of the hard repulsive core of the interparticle potential is significantly greater for p-H_2 (~ 3 Å) than it is for ^{4}He (~ 2.6 Å), The physical consequence is that, at

the equilibrium density of these two liquids, the hard core repulsion in p-H_2 is more effective at keeping particles apart, thereby drastically reducing the propensity to quantum-mechanical exchanges. An interesting question remains as to whether there actually does exist a sufficiently low temperature at which a (hypothetical) mestastable fluid phase of p-H_2 turns superfluid, or whether the possibility exists that this fluid may be normal all the way to $T = 0$. It is currently believed that *no* Bose system can be a non-superfluid liquid at $T=0$ [6]. This remains an outstanding issue.

CONCLUSIONS

Extensive simulation studies have been performed for a realistic model of p-H_2 adsorbed in the interior of a cylindrical channel of nanoscale size diameter. The results yield evidence that, although confinement can somewhat reduce the strong tendency of the system to crystallize, as observed in spherical cavities (Ref. [34]), nevertheless the effect is quantitatively more limited in a cylindrical geometry. Specifically, the predicted reduction of the Luttinger parameter K from its value in one dimension of 3.5, all the way to approximately 2 does not entail a fundamental change of the physical character of the system, which remains an insulator [75].

Consequently, any scheme aimed at stabilizing a bulk superfluid phase of p-H_2 in a network of interconnected cavities seems to face the hurdle that no superflow may be sustained inside narrow cylindrical channels connecting two adjacent cavities.

While the manuscript for Ref. [75] was undergoing review, we became aware of similar recent work [76], claiming that the value of the Luttinger parameter K can be lowered considerably with respect to what was found in this work, in fact to the point where p-H_2 could turn superfluid (in the Luttinger sense), inside Carbon nanotubes. The (cylindrical) geometry and diameters are similar to ours, but the model considered in Ref. [76] includes substrate

corrugation. These predictions, seemingly at variance with the results presented here, were obtained with a different computational methodology with respect to that utilized here, specifically a ground state one. Clearly, further studies will be needed to resolve this discrepancy.

A thorough numerical investigation was carried out of the possible superfluid properties of a hypothetical metastable fluid phase of p-H_2, of density equal to that of the freezing density, at temperatures below the freezing one, namely 13.8 K. Simulations were carried out down to a temperature $T=3$ K, significantly lower than that of the original prediction by Ginzburg and Sobyanin [11], and fairly close to the revised estimate by Apenko [13]. Simulations show a strong suppression of exchanges of identical molecules, with the ensuing failure of off-diagonal long range order (and therefore superfluidity) to set in. The lack of any significant temperature dependence of the physical behaviour observed in simulation leads to the conclusion that if a superfluid transition occurs, the transition temperature must be considerably lower than that currently estimated, at least by an order of magnitude. This conclusion is based on the expected similarity between p-H_2 and ^{4}He near the transition.

Because p-H_2 does not have a metastable superfluid phase in the $T \to 0$ limit, as shown by the results presented here, the window of temperature within which superfluidity of p-H_2 may be observable might well be very narrow, and in any case it is presently not accessible to available experimental methodology. The question of whether such a phase is obervable remains therefore open, but most of the avenues initially thought of do not seem viable, based on the current theoretical understanding.

Bibliography

[1] D. R. Tilley and J. Tilley, John Wiley and Sons Inc, New York, 1974.

[2] See, for instance, D. van Delft, *Freezing physics: Heike Kamerlingh Onnes and the quest for cold*, (Edita KNAW, Amsterdam, 2007).

[3] P. Kapitza, *Nature* **74**, 141 (1938).

[4] J. F. Allen and A. D. Misener, *Nature* **75**, 141 (1938).

[5] L. Tisza, *Nature* **141**, 913 (1938).

[6] See, for instance, A. Leggett, *Quantum Liquids*, (Oxford University Press, New York, 2006).

[7] See, for instance, R. P. Feynman, *Statistical Mechanics*, (Addison-Wesley, New York, 1972).

[8] D. M. Ceperley, *Rev. Mod. Phys.* **67**, 279 (1995).

[9] L. Reatto, D. E. Galli, M. Nava and M. W. Cole, J. Phys., Cond. Mat. **25**, 443001 (2013).

[10] See, for instance, C. J. Pethick and H. Smith, *Bose-Einstein Condensation in Dilute Gases*, (Cambridge University Press, Cambridge, 2002).

[11] Ginzburg, V. L. and Sobyanin, A. A. *JETP Lett.* **15**, 242 (1972).

[12] V.S. Vorob'ev and S.P. Malysehnko, *J. Phys. Cond. Mat.* **12**, 5071 (2000).

[13] S.M. Apenko, *Phys. Rev. B* **60**, 3052 (1999).

[14] There is no evidence of superfluidity in solid hydrogen. See, A. C. Clark, X. Lin, and M. H. W. Chan, *Phys. Rev. Lett.* **97**, 245301 (2006).

[15] For a general discussion of the possible occurrence of superfluidity in solid crystal, see, for instance, M. Boninsegni and N. Prokof'ev, *Rev. Mod. Phys.* **84**, 759 (2012).

[16] M. Kühnel, J. M. Fernández, G. Tejeda, A. Kalinin, S. Montero, and R. E. Grisenti, *Phys. Rev. Lett.* **106**, 245301 (2011).

[17] See, for instance, H. Wiechert, *Physics of Covered Solid Surfaces*, ed. by H. P. Bonzel (Springer, Berlin, 2003), Vol. 42 p. 166.

[18] M. Boninsegni, *Phys. Rev. B* **70**, 193411 (2004).

[19] M. Boninsegni, Phys. Rev. Lett. **111**, 235303 (2013).

[20] M. C. Gordillo and D. M. Ceperley, *Phys. Rev. Lett.* **79**, 3010 (1997).

[21] M. Boninsegni, *New J. Phys.* **7**, 78 (2005).

[22] J. Turnbull and M. Boninsegni, *Phys. Rev. B* **78**, 144509 (2008).

[23] M. Boninsegni, *Phys. Rev. B* **93**, 054507 (2016).

[24] J. L. Tell and H. J. Maris, *Phys. Rev. B* **28**, 5122 (1983).

[25] E. Molz, A. P. Y. Wong, M. H. W. Chan and J. R. Beamish, *Phys. Rev. B* **48**, 5741 (1993).

[26] It should also be mentioned that experimentally one observes the lowering of the superfluid transition temperature of liquid helium confined in vycor, i.e., confinement has also the effect of suppressing superfluidity. See, for instance, M. H. W. Chan, K. I. Blum, S. Q. Murphy, G. K. S. Wong and J. D. Reppy, *Phys. Rev. Lett.* **61**, 1950 (1988).

[27] G. Mason, *Proceedings of the Royal Society A: Mathematical, Physical and Engineering Sciences* **415**, 453 (1988).

[28] P. E. Sokol, R. T. Azuah, M. R. Gibbs and S. M. Bennington, *J. Low Temp. Phys.* **103**, 23 (1996).

[29] M. Bretz and A. L. Thomson, *Phys. Rev. B* **24**, 467 (1981).

[30] M. Schindler, A. Dertinger, Y. Kondo and F. Pobell, *Phys. Rev. B* **53**, 11451 (1996).

[31] P. Sindzingre, D. M. Ceperley, and M. L. Klein, *Phys. Rev. Lett.* **67**, 1871 (1991).

[32] F. Mezzacapo and M. Boninsegni, *Phys. Rev. Lett.* **97**, 045301 (2006).

[33] F. Mezzacapo and M. Boninsegni, *Phys. Rev. A* **75**, 033201 (2007).

[34] T. Omiyinka and M. Boninsegni, *Phys. Rev. B* **90**, 064511 (2014).

[35] F. D. M. Haldane, *Phys. Rev. Lett.* **47**, 1840 (1981)

[36] A. Del Maestro, M. Boninsegni, and I. R. Affleck, *Phys. Rev. Lett.* **106**, 105303 (2011).

[37] S. I. Shevchenko, Sov. *J. Low Temp. Phys.* **14**, 553 (1988).

[38] M. Boninsegni, A. B. Kuklov, L. Pollet, N. V. Prokof'ev, B. V. Svistunov, and M. Troyer, *Phys. Rev. Lett.* **99**, 035301 (2007).

[39] C. Chin, R. Grimm, P. Julienne, and E. Tiesinga, Rev. Mod. Phys. **82**, 1225 (2010).

[40] T. Omiyinka, M.Sc. Thesis, University of Alberta (2014).

[41] See, for instance, M. P. Allen, D. J. Tildesley, *Computer Simulation of Liquids*, (Clarendon Press, Oxford, 1989).

[42] See, for instance, J. J. Sakurai, *Modern Quantum Mechanics*, revised edition (Addison-Wesley, New York, 1994).

[43] V. Buch, *J. Chem. Phys.* **100**, 7610 (1994).

[44] I. S. Silvera, and V. V. Goldman, *J. Chem. Phys.* **69**, 4209 (1978).

[45] M. Moraldi, *J. Low Temp. Phys.* **168**, 275 (2012).

[46] T. Omiyinka and M. Boninsegni, *Phys. Rev. B* **88**, 024112 (2013).

[47] M. Boninsegni, N. Prokof'ev and B. Svistunov, *Phys. Rev. Lett.* **96**, 070601 (2006).

[48] M. Boninsegni, N. Prokof'ev and B. Svistunov, *Phys. Rev. E* **74**, 036701 (2006).

[49] R. P. Feynman. *Rev. Mod. Phys* **20**, 348 (1948).

[50] N. Metropolis, N. Rosenbluth, A. W. Rosenbluth, A. H. Teller and E. Teller, *J. Chem. Phys.* **21**, (1953) 1087-1092.

[51] R. P. Feynman and A. R. Hibbs, *Quantum Mechanics and Path Integrals*, (McGraw-Hills, Boston, 1967).

[52] Boninsegni M. *J. Low Temp. Phys.* **141**, 112 (2005).

[53] H. Flyvbjerg and H. G. Petersen, Error estimates on averages of correlated data, *J. Chem. Phys.* **91**, 461 (1989).

[54] We obtain ground state estimates by extrapolating to $T = 0$ low temperature results. In pratice, we have consistently found that the values of the energy values, as well as structural quantities (e.g., density profiles) remain unchanged, within statistical uncertainties, below a temperature $T \lesssim 4$ K.

[55] The value of the superfluid fraction of a finite system is obtained in a PIMC simulation using the "area" estimator. See P. Sindzingre, M. L. Klein and D, M. Ceperley, *Phys. Rev. Lett.* **63**, 1601 (1989).

[56] The probability distributions shown in Fig. 3.5 have only illustrative purpose. There is no known way of extracting from them the value of the superfluid fraction, which is directly computed by simulation using the "area" estimator, as mentioned above.

[57] L. Vranješ Markić and H. R. Glyde, *Phys. Rev. B* **92**, 064510 (2015).

[58] See, for instance, G. Stan, S. Gatica, M. Boninsegni, S. Curtarolo and M. W. Cole, Am. J. Phys. **67**, 1170 (1999), and references therein.

[59] G. J. Tjatjopoulos, D. L. Feke and J. A. Mann, *J. Phys. Chem.* **92**, 4006 (1988).

[60] The attractiveness of a wall potential depends both on the well depth D and on the distance of closest approach a. In the following, when speaking in general terms of "attractive strength" of a substrate, or anything equivalent, we shall always refer to a particular combination of values of D and a, not to the well depth D alone.

[61] A. Chizmeshya, M. W. Cole and E. Zaremba, *J. Low Temp. Phys.* **110**, 112 (1998).

[62] L. Pricaupenko and J. Treiner, *Phys. Rev. Lett.* **74**, 430 (1995).

[63] M. Boninsegni, *Phys. Rev. B* **70**, 125405 (2005).

[64] G. Vidali and M. W. Cole, *J. Low Temp. Phys.* **314**, Vol. 101 (1995).

[65] A Li substrate is known to display unusual adsorption properties precisely due to the fact that it is neither too weak nor too strong. For example, it is the weakest substrate on which a superfluid ^{4}He *mono*layer is predicted to exist. See M. Boninsegni, M. W. Cole and F. Toigo, *Phys. Rev. Lett.* **83**, 2002 (1999).

[66] M. Boninsegni, L. Pollet, N. Prokof'ev and B. Svistunov, *Phys. Rev. Lett.* **109**, 025302 (2012).

[67] The superfluid fraction is computed in a PIMC simulation by means of a specific estimator known as "winding number" estimator, introduced by D. Ceperley and E. Pollock in 1987. See, for instance, Ref. [8].

[68] L. H. Nosanow, L. J. Parish and F. J. Pinski, *Phys. Rev. B* **11**, 191 (1975).

[69] M. D. Miller, L. H. Nosanow and L. J. Parish, *Phys. Rev. B* **15**, 214.

[70] See, for instance, H. J. Maris, *Czech. J. Phys.* **46**, Suppl. 6, 2943 (1996).

[71] I. Silvera, Rev. Mod. Phys. **52**, 393 (1980).

[72] Although this result has been obtained using the Lennard-Jones potential, the same quantitative conclusion is reached using the Silvera-Goldman one. T. Omiyinka, unpublished (2016).

[73] It should be noted that at such low density the Silvera-Goldman and the modified Moraldi pair potential of Ref. [46] yield the same results, within statistical errors.

[74] Stated more quantitatively, the probability that a ^{4}He atom be involved in a cycle of exchanges with other ^{4}He atoms can be estimated at around 0.3%, at T=3 K and saturated vapour pressure (M. Boninsegni, unpublished). The equivalent quantity for p-H$_2$ at the same temperature, at the freezing density of the liquid, is estimated in this work at $< 10^{-8}$ (i.e., zero within the statistical uncertainty of the calculation).

[75] T. Omiyinka and M. Boninsegni, Phys. Rev. B **93**, 104501 (2016).

[76] M. Rossi and F. Ancilotto, ArXiv:1602.03282